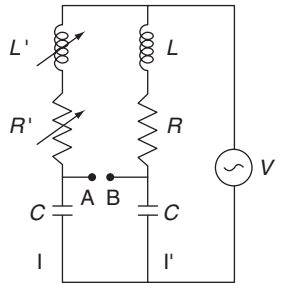

Figure W22.50. Ac bridge.

sample in the shape of a ring and winds N uniform turns of wire around it to fashion an inductor. The inductance is given by

$$L(\omega) = \frac{\mu_0 \mu_r(\omega) h N^2}{2\pi} \ln \frac{b}{a}, \tag{W22.169}$$

where it is assumed that the ring is in the form of an annulus of inner radius a, outer radius b, and thickness h. The inductance is seen to be a complex quantity and may be regarded as a pure inductor in series with a pure resistor. The reactance of the pair is $X = -i\omega L(\omega) = R - i\omega \text{ Re } (L(\omega)) \equiv R - i\omega L$, where

$$R = \frac{\omega \mu_0 \mu_2 h N^2}{2\pi} \ln \frac{b}{a}. \tag{W22.170}$$

The inductor is inserted into one leg of a bridge, as shown in Fig. W22.50. The other legs of the bridge consist of a variable inductor L' in series with a variable resistor R', and two capacitors, each with capacitance C. An ac voltage of frequency ω is imposed across the bridge. The value of R' and L' are adjusted until a null reading for the voltage occurs across the terminals A and B. The bridge is then balanced with $L' = L$ and $R' = R$. The values of $\mu_1(\omega)$ and $\mu_2(\omega)$ are then determined from Eqs. (W22.169) and (W22.170).

RESONANCE TECHNIQUES

The ability of scientists to determine resonance frequencies accurately has played a central role in the development of atomic and nuclear physics and gas-phase chemistry. The techniques were later applied to liquid-phase chemistry and ultimately to solid-state measurements. In the following sections several of these resonance techniques are described. The discussion begins with nuclear magnetic resonance spectroscopy. This is followed by a consideration of nuclear quadrupole resonance spectroscopy. Then electron spin resonance is studied. Finally, the Mössbauer effect is described.

W22.30 Nuclear Magnetic Resonance

It is possible to obtain useful information concerning the composition of a material and the local environment of its individual nuclei by performing nuclear magnetic

resonance (NMR) measurements. The procedure involves placing a sample of the material in a constant uniform magnetic field. A weak perturbing radio-frequency magnetic field is simultaneously applied to the sample while its frequency is varied until maximum power is delivered by the RF field to the sample. This frequency is called the *resonance frequency*. For a given magnetic field it is found that each nucleus has its own particular resonance frequency. The strength of the resonance is directly proportional to the amount of that particular nucleus present in the sample. This is the basis of the use of NMR as a tool for determining the chemical composition. In addition, there are slight shifts of the resonance frequency caused by variations of the local chemical environment of the nucleus. This is due to the nuclei coupling to the surrounding electrons by magnetic interactions and the electrons also coupling to the applied magnetic field. Since the electron distribution reflects the chemical environment (e.g., which chemical bonds are present and what the NNs and next-NNs are), one may also use NMR to obtain this kind of information as well. From a knowledge of the NNs and next-NNs one is often able to piece together the structure of complicated chemical compounds or solids. The utility of NMR hinges on the ability to generate uniform magnetic fields and to perform resonance measurements with extremely high precision. The utility is also based on having a database of NMR signals from known sequences of atoms with which a comparison may be made in determining the structure of a complex molecule or solid.

Some of the main features of NMR follow directly from a classical-mechanical theory, although the correct description must be formulated within the framework of quantum mechanics. The need for a quantum theory stems from the fact that angular momentum is quantized. A nucleus has an angular momentum operator given by

$$\mathbf{J} = \mathbf{I}\hbar, \tag{W22.171}$$

where $\mathbf{I}$ is a vector of spin matrices (i.e., I_x, I_y, and I_z are square matrices). The magnitude of the angular momentum, according to quantum mechanics, is given by $\hbar[I(I+1)]^{1/2}$, where I is either a nonnegative integer or a half integer. The number of rows in the matrices I_x, I_y, or I_z is $2I+1$. For nuclei, I is small and quantum effects are important. For pedagogic reasons, however, the discussion begins with the classical theory. The quantum-mechanical treatment is covered in Appendix W22A.

A nucleus has a magnetic moment directed along the spin angular momentum vector

$$\mathbf{m} = g_I \mu_N \hbar \mathbf{I} = \hbar \gamma \mathbf{I}, \tag{W22.172}$$

where $\mu_N = e\hbar/2M_p = 5.050824 \times 10^{-27}$ J/T is the nuclear magneton, g_I is the nuclear g factor, and $\gamma = g_I \mu_N$. Each nucleus has its unique value of γ, and this is what gives NMR its chemical (and isotopic) specificity. Impose a uniform magnetic induction $\mathbf{B} = B_0 \hat{k}$ on the nucleus. The nucleus will experience a magnetic torque and this will cause the spin angular momentum to change its direction in time according to

$$\frac{d\mathbf{I}}{dt} = \frac{\mathbf{m} \times \mathbf{B}}{\hbar} = \gamma B_0 \, \mathbf{I} \times \hat{k} = \mathbf{I} \times \boldsymbol{\Omega}. \tag{W22.173}$$

This is in the form of a precession equation for $\mathbf{I}$. The precession frequency is the magnitude of the vector

$$\boldsymbol{\Omega} = \frac{\gamma \mathbf{B}}{\hbar}. \tag{W22.174}$$

TABLE W22.3 Spin $I = \frac{1}{2}$ Nuclei Commonly Used in NMR Spectroscopy

Nucleus	Isotopic Abundance (%)	f ($B = 1$ T) (MHz)
^{1}H	99.985	42.5764
^{13}C	1.10	10.7081
^{15}N	0.366	4.3172
^{19}F	100	40.0765
^{29}Si	4.67	8.4653
^{31}P	100	17.2510
^{89}Y	100	2.0949
^{109}Ag	48.161	1.9924
^{119}Sn	8.59	15.9656
^{183}W	14.3	1.7956
^{199}Hg	16.87	7.7121
^{205}Tl	70.476	24.9742
^{207}Pb	22.1	9.0338

Source: D. R. Lide, ed., *CRC Handbook of Chemistry and Physics*, 75th ed., CRC Press, Boca Raton, Fla., 1997.

A list of some nuclei commonly used in NMR, along with their precession frequencies, $f = \Omega/2\pi$ is given in Table W22.3. Many nuclei have $I = 0$ and so are not NMR-active (e.g., ^{12}C, ^{16}O, ^{28}Si, ^{56}Fe).

The effect of the electrons, which are sensitive to the chemical environment, is to partially shield the nucleus from the magnetic field. The magnetic induction may be written as

$$\mathbf{B} = (\overleftrightarrow{I} - \overleftrightarrow{\sigma}) \cdot \mathbf{B}_0, \tag{W22.175}$$

where $\overleftrightarrow{\sigma}$ is called the *shielding tensor*. It may be written as the sum of an isotropic part, $\sigma\overleftrightarrow{I}$, and an anisotropic part, $\Delta\overleftrightarrow{\sigma}$ (i.e., $\overleftrightarrow{\sigma} = \sigma\overleftrightarrow{I} + \Delta\overleftrightarrow{\sigma}$). The effect of the shielding is usually described in terms of a chemical-shift parameter, δ. The value is usually reported relative to a standard value

$$\delta = \frac{\Omega - \Omega_{\text{st}}}{\Omega_{\text{st}}} \times 10^6, \tag{W22.176}$$

where Ω_{st} is the frequency of the standard. The frequency shifts for protons typically range from 0 to 10 ppm. For ^{13}C they range up to ≈ 200 ppm. The standard used is often the tetramethylsilane (TMS) molecule, $(CH_3)_4Si$.

If the precession equation is separated into components, three equations are obtained:

$$\frac{dI_x}{dt} = \Omega I_y, \qquad \frac{dI_y}{dt} = -\Omega I_x, \qquad \frac{dI_z}{dt} = 0. \tag{W22.177}$$

It follows that I_z and I remain constant in time. The x and y components undergo a precessional motion

$$I_x = I_0 \cos \Omega t, \qquad I_y = -I_0 \sin \Omega t, \tag{W22.178}$$

where I_0 is a constant in the classical theory. The value of I_z is that appropriate to thermal equilibrium, and is given in terms of the Brillouin function:

$$\langle I_z \rangle = IB_I \left(\frac{\gamma IB}{k_B T} \right), \tag{W22.179}$$

which is analogous to Eqs. (9.23) and (9.24).

In a solid, the nuclei interact with the other atoms of the material through a variety of interactions, including spin–orbit and spin–spin interactions. These interactions have two effects. First, they cause the z component of the nuclear spin to relax to its equilibrium value, with a characteristic relaxation time T_1, that is,

$$\frac{dI_z}{dt} = -\frac{I_z - \langle I_z \rangle}{T_1}. \tag{W22.180}$$

The parameter T_1 is called the *longitudinal* or *spin-lattice relaxation time*. Second, they cause the precessional motion to become phase interrupted. Introduce a phenomenological damping term to account for this spin–lattice interaction:

$$\frac{dI_x}{dt} + \frac{I_x}{T_2} = (\mathbf{I} \times \Omega)_x, \tag{W22.181}$$

$$\frac{dI_y}{dt} + \frac{I_y}{T_2} = (\mathbf{I} \times \Omega)_y, \tag{W22.182}$$

The parameter T_2 is called the *transverse relaxation time*. It is assumed that there is no difference in the phase-interruption time constant for x- or y-spin components.

It is convenient to form the combination $I_+ = I_x + iI_y$ and combine the two precession equations into one:

$$\left(\frac{d}{dt} + i\Omega + \frac{1}{T_2} \right) I_+ = 0. \tag{W22.183}$$

This is an equation for damped oscillation of the spin.

Next, introduce the perturbing magnetic field, $\mathbf{H}'(t)$, at right angles to $\mathbf{B}$. It is taken to be circularly polarized, since this leads to a simpler formula. Thus

$$H'_x = H' \cos \omega t, \qquad H'_y = -H' \sin \omega t. \tag{W22.184}$$

The dynamical equation becomes

$$\left(\frac{d}{dt} + i\Omega + \frac{1}{T_2} \right) I_+ = i\Omega' I_z \exp(-i\omega t), \tag{W22.185}$$

where $\Omega' = \mu_0 \gamma H'/\hbar$. In the limit of weak RF fields, I_x and I_y will be small, so I_z will differ from $\langle I_z \rangle$ only by terms of order $(H')^2$. Hence I_z will be approximated by $\langle I_z \rangle$. A steady-state solution for I_+ is found by writing $I_+ = I_0 \exp(-i\omega t)$, so

$$I_0 = \frac{\Omega' \langle I_z \rangle}{\Omega - \omega - i/T_2}. \tag{W22.186}$$

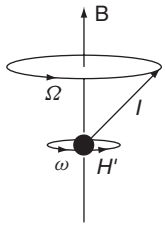

Figure W22.51. Precession of a nuclear spin around the magnetic-induction vector.

This equation demonstrates that as the frequency ω approaches the resonance frequency Ω, the amplitude of I_+ can grow to be large, limited only by the shortness of T_2. The resonance is detected by monitoring the power transfer from the RF circuit to the spin system. It shows up by adding extra inductance and resistance to the RF circuit. This power, of course, is ultimately transferred to the translational motion of the other atoms and so heats the material. A sketch of the precessing magnetic dipole is presented in Fig. W22.51.

The resonance frequency of a nucleus depends on the *local* magnetic field. In addition, for spin $I \geq 1$, nuclei also possess electric-quadrupole moments. These interact with electric fields and affect the NMR spectrum in important ways. The local magnetic field is given by the sum of the applied field and the fields due to all the other electronic and nuclear magnetic moments of the material. Since these moments are likely to be oriented in an almost random manner, each nucleus will experience a different magnetic field and hence have a different resonance frequency. Instead of the sample exhibiting a sharp NMR resonance line, the line will be inhomogeneously broadened. It is important to make a distinction between the magnetic moments participating in the resonance (such as protons interacting with other protons in an proton NMR signal) and other moments (such as protons interacting with Fe atomic spins in iron). In this example, the spin–spin interaction of the protons is approximately included in the parameter T_2. The other interactions contribute to the inhomogeneous broadening of the NMR line. This limits the ability to resolve closely spaced resonance lines.

There are at least two methods to overcome this limitation. One may do NMR on a liquid instead of a solid. There is a phenomenon called *motional line narrowing* which can occur in liquids and will now be explained. As the nuclei move about due to their thermal motion, the contribution to the local magnetic field from other nuclei is as likely to be in one direction as in the opposite direction. Its average value is zero, although the mean-square fluctuation remains nonzero. Let the contribution to the precession frequency of a given nucleus from the other magnetic dipoles of the material be denoted by $\Omega''(t)$. As a simple model, suppose that it may assume only two values, $+\Omega''$ and $-\Omega''$, and that there is a 50% probability of switching from one value to the other every τ seconds. The mean value of the square of the accumulated phase after a time t is then

$$\overline{\left[\int_0^t \Omega''(t')\,dt'\right]^2} = \frac{t}{\tau}\Omega''^2\tau^2, \tag{W22.187}$$

where t/τ is the number of opportunities for switching that occur. If the effective dephasing time is determined by when this is ≈ 1 radian, an estimate for T_2 is obtained:

$$T_2 = \frac{1}{\Omega''^2 \tau}. \tag{W22.188}$$

As the thermal motion increases, τ becomes smaller and the dephasing time becomes longer.

A second technique for reducing the inhomogeneous width is called *magic-angle spinning*. It permits high-resolution NMR to be applied to solid-state samples. It may be accomplished by either actually physically spinning the solid about an axis making an angle $\theta = 54.7^\circ$ with the dc magnetic field and using a very weak RF field, or holding the sample stationary but arranging that the ratio of the RF magnetic field to the dc magnetic field be equal to $H'/H_0 = \tan(54.7^\circ) = 2^{1/2}$. To understand how this comes about, consider the magnetic dipole–dipole interaction between the magnetic dipoles located at the various sites $\mathbf{r}_i$ in the solid:

$$U = \frac{\mu_0}{4\pi} \sum_{i=1}^{N} \sum_{j=i+1}^{N} \frac{3(\mathbf{m}_i \cdot \hat{r}_{ij})(\mathbf{m}_j \cdot \hat{r}_{ij}) - \mathbf{m}_i \cdot \mathbf{m}_j}{r_{ij}^3}, \tag{W22.189}$$

where $r_{ij} = |\mathbf{r}_i - \mathbf{r}_j|$. It will be assumed that the magnetic field is strong enough so that $\mathbf{m}_i$ precesses rapidly around the applied magnetic induction $\mathbf{B}_0$. On the average, the magnetic moment therefore points along the direction of the magnetic field. The angular factor in the numerator may then be written as

$$2P_2(\cos\theta_{ij}) = 3\cos^2\theta_{ij} - 1 = 3(\hat{B}_0 \cdot \hat{r}_{ij})^2 - 1, \tag{W22.190}$$

where $P_2(\cos\theta)$ is the second-order Legendre polynomial. Now suppose that the solid is spun around some axis with an angular velocity Ω_s (Fig. W22.52). There is an identity, called the *addition theorem for spherical harmonics*,

$$P_L(\cos\theta_{ij}) = \frac{4\pi}{2L+1} \sum_{M=-L}^{L} Y_{LM}^*(\theta, \phi) Y_{LM}(\psi_{ij}, \phi_{ij}), \tag{W22.191}$$

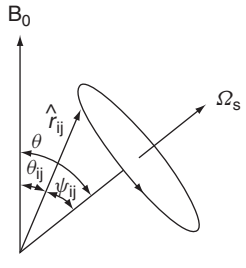

Figure W22.52. Orientation of the external magnetic field, $\mathbf{B}_0$, the displacement unit vector, $\hat{r}_{ij}$, and the rotation velocity, Ω_s.

where the Y_{LM} are spherical harmonics and ϕ denotes an azimuthal angle (not shown in the figure) around vector $\mathbf{\Omega}_s$. In the course of the angular motion, the terms involving $M \neq 0$ average out, so

$$P_2(\cos\theta_{ij}) \longrightarrow P_2(\cos\psi_{ij})P_2(\cos\theta). \tag{W22.192}$$

If $\cos^2\theta = \frac{1}{3}$ (i.e., $\theta = 54.7^\circ$), then $P_2(\cos\theta) = 0$ and the spin–spin interaction is effectively removed as a first-order perturbation in the problem. This allows the lines to become very narrow when the solid is spun at the magic angle. It must be emphasized, however, that magic-angle spinning is only effective in eliminating the broadening due to "like" spins. It does not eliminate inhomogeneous broadening due to other sources.

It is possible to remove some dipole–dipole broadening effects due to the interactions between unlike spins by employing a technique called *dipolar decoupling*. For example, suppose that ^{1}H is present and one is interested in studying the ^{13}C spectrum. Normally, the two spins would interact in such a way as to broaden the spectra. A strong RF field is applied whose frequency resonates with the protons. The spins of the protons are made to flip up and down rapidly and hence their magnetic moments average to zero. Their interaction with the ^{13}C nuclei is suppressed.

It is also possible to use a technique called *cross-polarization* to increase the sensitivity of the NMR resonance of one of the spins of a multispin system. For example, there may be many more ^{1}H nuclei present than ^{13}C nuclei. In this technique one applies two RF frequencies which effectively lock the nuclear resonances together. This occurs when the Hahn–Hartmann condition applies (i.e., $\gamma_C B_C = \gamma_H B_H$). The Zeeman splittings of the two nuclei are made degenerate with each other, and this facilitates the resonant exchange of energy via the spin–spin interaction. The net result is a transfer of magnetization from the majority ^{1}H nuclei to the minority ^{13}C nuclei and a strengthening of the ^{13}C signal.

It should also be mentioned that in some solids the analysis of the NMR line shape reveals that the interaction between "like" spins leads to non-Lorentzian resonances. This reflects a limitation of the Bloch equations in which one attempts to parametrize all dephasing effects in terms of a single time, T_2. The measured line shape may contain important information concerning the interatomic distances and the short-range order, in general.

The relaxation time T_1 can be very long, in the range of minutes or longer. In some cases this long relaxation time limits the ability to carry out NMR experiments on solids. On the other hand, it also implies that quantum coherence is being maintained for a long period of time. This could potentially be utilized in the construction of quantum computers, which rely on the quantum-mechanical coherence being maintained during the course of a calculation.

NMR is a long-established technique and there are a variety of ways of employing it. There are powerful methods using time-programmed pulses of RF magnetic fields, but these will not be discussed here.

It is also possible to obtain information concerning the density of conduction electrons by measuring the Knight shift. At a given frequency the nuclear magnetic resonance of a nucleus in a metal occurs at a different value of the magnetic field than it would in an insulator. The Knight shift is defined as $-\Delta B/B$. This is due to the fact that the conduction electrons exhibit magnetism, and this modifies the local magnetic field experienced by the nucleus. The interaction responsible for this shift (called the

Fermi contact interaction) is a point-magnetic interaction between the electron-spin magnetic moment and the magnetic moment of the nucleus. An expression for this interaction may be obtained by regarding the nucleus as a small magnetized sphere of radius b and allowing the size of the sphere to shrink to zero. The magnetic induction inside the sphere can be shown, by elementary magnetostatic arguments, to be given by $\mathbf{B}_{\text{in}} = \mu_0 g_I \mu_N \mathbf{I}/2\pi b^3$. The interaction energy is $V = g_e \mu_B \mathbf{s} \cdot \mathbf{B}_{\text{in}}$, so

$$V = \frac{2\mu_0}{3} g_e \mu_B g_I \mu_N \mathbf{s} \cdot \mathbf{I} \delta(\mathbf{r}), \tag{W22.193}$$

g_e being the electron g factor and μ_B the Bohr magneton. The substitution $1/(4\pi b^3/3) \rightarrow \delta(\mathbf{r})$ is also made in deriving this formula. Applying first-order perturbation theory, one finds an expression for the energy of the nuclear magnetic moment in the magnetic field:

$$E = -g_I \mu_N \mathbf{I} \cdot \left[\mathbf{B} - \frac{2\mu_0}{3} g_e \mu_B \mathbf{s} |\psi(0)|^2 \right], \tag{W22.194}$$

where $|\psi(0)|^2$ is the probability density for finding the electron at the nucleus. The Knight shift, K, is therefore

$$K \equiv -\frac{\Delta B}{B} = \frac{2\mu_0 g_e \mu_B \langle s_z \rangle}{3B} |\psi(0)|^2. \tag{W22.195}$$

This may be expressed in terms of the magnetic susceptibility χ and the magnetic permeability μ using the relation $\langle s_z \rangle / B = \chi / n \mu_0 g_e \mu_B$, where n is the electron density. Typical experimental values for the Knight shift for the alkali metals ^{7}Li, ^{23}Na, ^{39}K, and ^{87}Rb are 0.026%, 0.112%, 0.265%, and 0.653%.

The Fermi contact interaction is also responsible for the relaxation of the z component of the spins. Korringa derived a relation for the spin–lattice relaxation time, based on Fermi's golden rule, in terms of the Knight shift in metals:

$$T_1 \left(\frac{\Delta B}{B} \right)^2 = \frac{\hbar g_e^2 \mu_B^2}{4\pi k_B T g_I^2 \mu_N^2} = \frac{\hbar g_e^2 M_p^2}{4\pi k_B T g_I^2 m_e^2}. \tag{W22.196}$$

In Fig. W22.53 magic-angle spinning NMR spectra are presented for ^{29}Si at 79.5 MHz from samples of the catalyst ZSM-5 discussed in Section 13.6. The spectra are compared for various degrees of removal of Al from the framework. The NMR spectra are far more sensitive to the changes in the lattice structure than are x-ray diffraction spectra. A precise determination of the lattice geometry may be obtained from NMR studies.

W22.31 Nuclear Quadrupole Resonance

Nuclei with spins greater than or equal to $\frac{1}{2}$ possess magnetic moments. If the spins are greater than 1, they also possess electrical-quadrupole moments. The quadrupole moment is a measure of the spherical asymmetry of the charge distribution of the

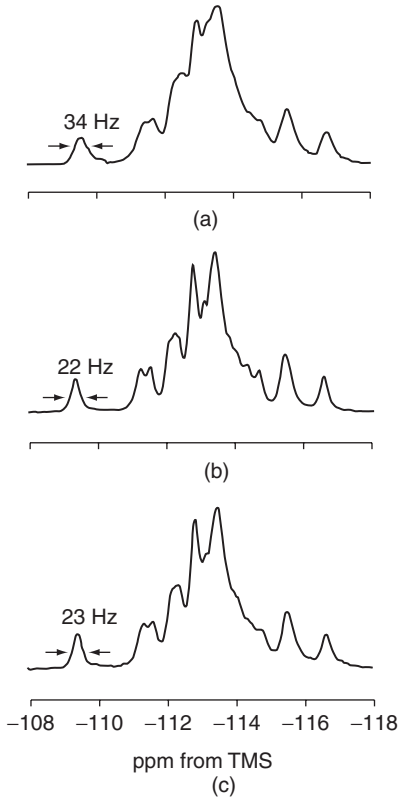

Figure W22.53. ^{29}Si magic-angle spinning NMR spectra for the zeolite ZSM-5 for various degrees of dealumination. The Si/Al ratios are: (*a*), 20; (*b*), 125; (*c*), 800. [Reprinted with permission from C.A. Fyfe et al., *J. Phys. Chem.*, **88**, 3248 (1984). Copyright 1984 by the American Chemical Society.]

nucleus. The quadrupole moment is defined in terms of the nuclear charge density $\rho(\mathbf{r})$ by

$$eQ = \int d\mathbf{r}\, \rho(\mathbf{r})(3z^2 - r^2), \tag{W22.197}$$

where the z axis is directed along the spin angular momentum vector. The sign of Q is an indicator of the shape of the nucleus, being positive for cigar-shaped nuclei and negative for pancake-shaped nuclei. Nuclei do not possess electric-dipole moments, consistent with the invariance of the strong interaction under parity reversal (and also time reversal).

The interaction of a quadrupole moment with an inhomogeneous electric field is obtained from a Taylor series expansion:

$$U = \int d\mathbf{r}\Phi(\mathbf{r})\rho(\mathbf{r}) = Ze\Phi(0) + \frac{e}{6}\sum_{\alpha,\beta}\frac{\partial^2\Phi}{\partial x_\alpha \partial x_\beta}Q_{\alpha\beta} + \cdots, \tag{W22.198}$$

where $\Phi(\mathbf{r})$ is the electrostatic potential and Z is the atomic number of the nucleus. The coefficients $Q_{\alpha\beta}$ define what is called the *quadrupole tensor*:

$$eQ_{\alpha\beta} = \int d\mathbf{r}\, \rho(\mathbf{r})(3x_\alpha x_\beta - r^2\delta_{\alpha\beta}). \tag{W22.199}$$

It is defined here so that it has the dimensions m^2 and is represented by a symmetric matrix. The only vector defined for the nucleus as a whole is the spin angular-momentum vector. Therefore, all vectors can be expressed in terms of $\mathbf{I}$, so

$$\int d\mathbf{r}\, \rho(\mathbf{r})x_\alpha x_\beta = \frac{C}{2}(I_\alpha I_\beta + I_\beta I_\alpha), \qquad \int d\mathbf{r}\, \rho(\mathbf{r})r^2 = CI^2. \tag{W22.200}$$

If the expectation values of these expressions are evaluated in the state in which $\mathbf{I}^2|I, I\rangle = I(I+1)|I, I\rangle$ and $I_z|I, I\rangle = I|I, I\rangle$, then C may readily be shown to be equal to

$$C = \frac{eQ}{I(2I-1)}. \tag{W22.201}$$

The product of the spin matrices has been written in a form that preserves the symmetry of the quadrupole tensor. (Note that angular momenta matrices need not commute with each other.) The Hamiltonian for the quadrupole interaction is

$$H_Q = \frac{C}{6}\sum_{\alpha\beta}\Phi_{\alpha\beta}\left[\frac{3}{2}(I_\alpha I_\beta + I_\beta I_\alpha) - \delta_{\alpha\beta}I^2\right], \tag{W22.202}$$

using a shorthand notation for the second derivative of the potential. After some manipulation and making use of $\nabla^2\Phi = 0$, this reduces to

$$H_Q = \frac{e^2Qq}{4I(2I-1)}\left[3I_z^2 - I^2 + \eta(I_x^2 - I_y^2)\right], \quad \Phi_{zz} \equiv eq, \quad \frac{\Phi_{xx} - \Phi_{yy}}{\Phi_{zz}} \equiv \eta, \tag{W22.203}$$

where η is called the asymmetry parameter and eqQ is called the *quadrupole-coupling parameter*. The effects of this interaction are probed in NQR experiments.

This equation shows how the nuclear spin couples to the gradient of the electric field. This field is set up by the neighboring ions and their associated electron charge distributions. The field depends on the types of neighboring atoms, the internuclear distances, and the types of chemical bonds that are formed. NQR therefore provides a useful tool for obtaining the information above.

It is not possible to create strong-enough RF laboratory electric-field gradients that can be used as the basis for NQR resonance measurements. Instead, one uses the RF magnetic field, usually in conjunction with a dc magnetic field, and looks at the simultaneous NMR and NQR effects. For example, suppose that there is a dc magnetic field directed along the z axis, and this is aligned with a symmetry axis of the crystal. In this case, $\eta = 0$. The Hamiltonian then consists of a Zeeman term and the quadrupole interaction:

$$H = -\gamma B_0 I_z + \frac{e^2Qq}{4I(2I-1)}(3I_z^2 - \mathbf{I}^2). \tag{W22.204}$$

The first-order splitting caused by such an interaction may be obtained for the eigenstates $|I, m\rangle$ as

$$\langle I, m|H|I, m\rangle = -\hbar\gamma B_0 m + \frac{e^2Qq}{4I(2I-1)}[3m^2 - I(I+1)]. \tag{W22.205}$$

The effect of the Zeeman term is to lift the degeneracy by spreading out the sublevels uniformly. The effect of the quadrupole coupling is to raise (or lower) states with $\pm m$ by the same amount. The combined effect is to produce a nonuniform spreading of the sublevels. The magnetic-dipole selection rule is $\Delta m = \pm 1$. The transitions may be tracked in a resonance experiment, and the value of eqQ may be obtained to high precision.

For the case where there is no axial symmetry the formulas are more complicated. For $I = 1$ one finds that

$$\langle 1, m|H|1, m\rangle = \begin{cases} -\dfrac{e^2}{2}qQ & \text{if} \quad m = 0, \\ \mp\gamma B_0 + \dfrac{e^2qQ}{4}(1 \pm \eta), & \text{if} \quad m = \pm 1, \end{cases} \tag{W22.206}$$

and for $I = \frac{3}{2}$ one finds that

$$\left\langle \frac{3}{2}, m|H|\frac{3}{2}, m\right\rangle = \begin{cases} \mp\dfrac{\gamma B_0}{2} + \dfrac{e^2}{4}qQ\sqrt{1+\eta^2/3}, & \text{if} \quad m = \pm\dfrac{1}{2}, \\ \mp\dfrac{3\gamma B_0}{2} - \dfrac{e^2qQ}{4}\sqrt{1+\eta^2/3}, & \text{if} \quad m = \pm\dfrac{3}{2}. \end{cases} \tag{W22.207}$$

Typical values of Q are presented in Table W22.4, along with nuclear spins, abundances, and Zeeman (precession) frequencies for magnetic-dipole transitions. Nuclear quadrupole resonance provides information about bond hybridization and the covalent nature of the chemical bond. For example, if there is sp-hybridization, only the p-orbital contributes to the quadrupole moment. Similarly, in ionic bonding, the closed-shell ions do not possess quadrupole moments.

TABLE W22.4 Spins, Abundances, Precession Frequencies, and Quadrupole Moments for Some Nuclei

Nucleus	Spin I	Isotopic Abundance (%)	$f(B = 1\ \text{T})$ (MHz)	Q (10^{-30} m^2)
^{2}H	1	0.015	42.5764	0.2860
^{11}B	$\frac{3}{2}$	80.1	13.6626	4.059
^{17}O	$\frac{5}{2}$	0.038	5.7741	−2.558
^{25}Mg	$\frac{5}{2}$	10.00	2.6082	19.94
^{27}Al	$\frac{5}{2}$	100	11.1028	14.03

Source: Data from D. R. Lide, ed., *CRC Handbook of Chemistry and Physics*, 75th ed., CRC Press, Boca Raton, Fla., 1997.

W22.32 Electron-Spin Resonance

Much of the inner workings of atoms has been elucidated by employing resonance techniques in conjunction with the use of external magnetic fields. The physics of the atom is described in terms of a succession of contributions to the Hamiltonian. These describe the kinetic energy, the electrostatic interaction between the electrons and the nucleus, the electron–electron electrostatic interactions, the spin–orbit coupling, the spin–spin interaction, the interaction of the electron orbital angular momentum $\mathbf{L}$ and spin $\mathbf{S}$ with external magnetic fields, the hyperfine interaction, the nuclear Zeeman and quadrupole couplings, and various relativistic and quantum-electrodynamic corrections. If the atom is not free but is embedded in a crystal, one must, in addition, consider the effect of the crystal electric field imposed by the neighboring ions and electrons, the interaction of the atomic spin with the spins on nearby atoms, and the possibility of losing electrons to or gaining electrons from other atoms of the solid. These effects are often by no means small and lead to major perturbations of the energy levels and the corresponding spectroscopy. To the extent that they can be understood, however, they provide a powerful analytical tool for probing the solid. The field is called *electron-spin resonance* (ESR) or sometimes *electron paramagnetic resonance* (EPR). For simple electron-spin systems, ESR may be described in terms of the Bloch equations, although the quantum-mechanical approach is used in this section.

ESR is a very rich field and cannot be summarized adequately in a short amount of space. It can provide information concerning donor or acceptor impurities in semiconductors. It can be used to study transition metal ions. It is useful for analyzing color centers in insulators. It is sensitive to electron and hole traps. There are two simple uses for it: determining the symmetry of the site where the spin sits and determining the valence of the magnetic ion.

In atomic physics one is concerned with the coupling of the nuclear spin, $\mathbf{I}$, to the electronic spin, $\mathbf{J} = \mathbf{L} + \mathbf{S}$, to form a total angular momentum $\mathbf{F} = \mathbf{I} + \mathbf{J}$. In the presence of a magnetic induction $\mathbf{B} = \hat{k}B_0$, the Hamiltonian for a given electronic term is written as

$$H = \lambda \mathbf{L} \cdot \mathbf{S} + \mu_B \mathbf{B} \cdot (\mathbf{L} + g\mathbf{S}) + A\mathbf{S} \cdot \mathbf{I} + \mu_N \mathbf{B} \cdot \mathbf{I}, \tag{W22.208}$$

where the first term is the spin–orbit coupling, the second term is the electronic Zeeman effect, the third term represents the hyperfine coupling, and the last term is the nuclear Zeeman effect (which is three orders of magnitude weaker). The parameter g is the g factor of the electron and is approximately 2. One usually forms matrix elements of this Hamiltonian in an appropriate basis, diagonalizes the matrix, and interprets the eigenvalues as the energy levels. Resonance spectroscopy may then be used to drive transitions between the energy levels and therefore to deduce the coupling constants, λ and A, as well as to determine L, S, and I.

The same basic idea is used in the solid, but the Hamiltonian becomes more complicated. First, quenching of the orbital angular momentum may occur. This occurs in the sp-bonded materials and transition metal ions (but not in the rare earths with f electrons, which need to be considered separately). Since the crystal is not an isotropic medium, the mean orbital angular momentum operator does not commute with the potential energy function. On the other hand, to a first approximation, the electron and nuclear spins are impervious to the presence of this anisotropy. In place of the full rotational symmetry of the free atom, there is the point-group symmetry of the crystal.

A fruitful approach is to try to write a Hamiltonian operator involving **S**, **I**, and **B** in a form that will respect the symmetry operations of the crystal. This will often require introducing more than two arbitrary constants. Resonance techniques are able to determine these parameters in the same way as they are determined for a free atom. The size of the parameters often offers important clues to the nature of the chemical bonds formed. Moreover, a study of the degeneracies and their lifting under the application of a magnetic field allows valuable information concerning the valency and symmetry of the paramagnetic ions to be obtained.

As an example, consider the case of a magnetic ion sitting on a site with octahedral symmetry inside a cubic host crystal. The Hamiltonian may be written as

$$H = g\mu_B \mathbf{B} \cdot \mathbf{S} + A\mathbf{S} \cdot \mathbf{I} + C(S_x^4 + S_y^4 + S_z^4) + D(S_x^6 + S_y^6 + S_z^6) + \cdots, \quad \text{(W22.209)}$$

where the higher-order terms are usually smaller than the lower-order terms and are often neglected. This Hamiltonian respects the cubic symmetry of the crystal in that the permutation $x \to y \to z \to x$ is a symmetry operation (rotations of 120° around the main diagonal), as is $x \to -x$ (reflections in bisecting planes), $(x, y) \to (y, -x)$ (90° rotations), and so on.

Now suppose that a tetragonal distortion is introduced in the crystal. The x and y lattice constants are assumed to remain the same, but the z lattice constant is made different. This introduces new parameters into the Hamiltonian:

$$\begin{aligned} H = {} & g_z\mu_B S_z B_z + g_{xy}\mu_B[S_x B_x + S_y B_y] + A_z S_z I_z \\ & + C' S_z^2 + A_{xy}[S_x I_x + S_y I_y] + P\left[I_z^2 - \tfrac{1}{3}I(I+1)\right], \end{aligned} \quad \text{(W22.210)}$$

where higher-order terms have been dropped.

If the symmetry is lifted further, by creating an orthorhombic distortion, the Hamiltonian is expanded even further:

$$\begin{aligned} H = {} & g_z\mu_B S_z B_z + g_x\mu_B S_x B_x + g_y\mu_B S_y B_y + A_z S_z I_z + A_x S_x I_x + A_y S_y I_y \\ & + P[I_z^2 - \tfrac{1}{3}I(I+1)] + C' S_z^2 + C''(S_x^2 - S_y^2). \end{aligned} \quad \text{(W22.211)}$$

A typical lifting of the degeneracy is represented in Fig. W22.54 for the case of a d-shell electron. The ten-fold degenerate level for the free ion is split in stages and ultimately consists of five doubly degenerate levels.

In Fig. W22.55 results are presented for a Mn^{2+} ion in a calcite host crystal, $CaCO_3$. In the presence of the magnetic field the $S = 5/2$ level is Zeeman-split into $2I + 1 = 6$ lines. The widths of the lines are attributed mainly to random strains in the crystal.

W22.33 Mössbauer Spectroscopy

Consider the gamma decay of an isolated radioactive nucleus in an excited state I resulting in a ground-state nucleus F. A gamma ray of energy $\hbar\omega$ is emitted in one direction and nucleus F recoils with momentum $\hbar\omega/c$ in the opposite direction. The total energy available in the transition is the sum of the photon energy and the recoil energy: $E = \hbar\omega + (\hbar\omega)^2/2Mc^2$, where M is the nuclear mass. The photon that is emitted cannot be absorbed by another F nucleus, because it is shifted out of resonance (i.e., $\hbar\omega < E$).

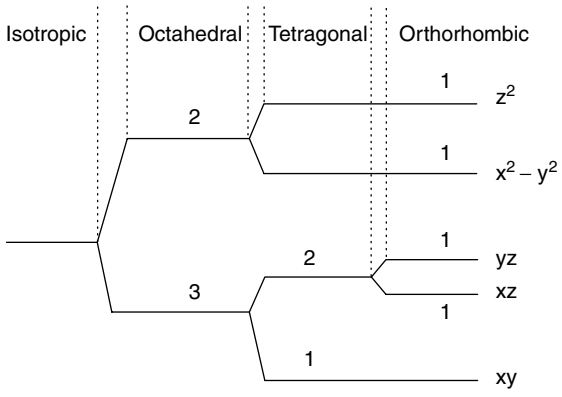

Figure W22.54. Lifting of the degeneracy of the *d*-electron energy levels as the symmetry of the crystal is lowered.

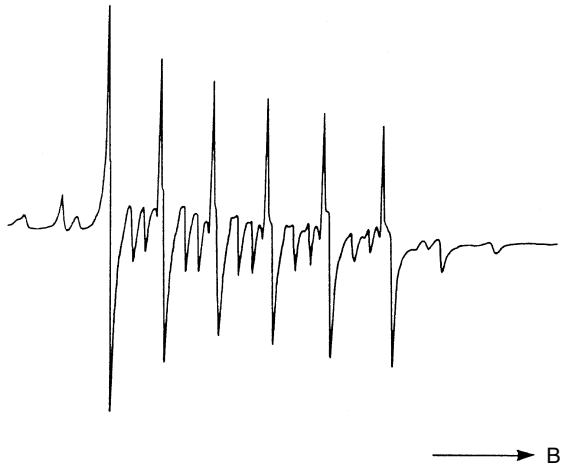

Figure W22.55. ESR spectrum of a Mn^{2+} ion in a calcite host. [Reprinted from J. G. Angus et al, *Chem. Geol.*, **27**, 181 (1979). Copyright 1979, with permission from Elsevier Science.]

The natural width of the emission line, determined by its radiative lifetime, is typically on the order of several 10^{-9} eV, much smaller than the recoil energy. There are only several nuclei that may be used in Mössbauer spectroscopy. Chief among them is ^{57}Fe. The parent nucleus is ^{57}Co. The sequence of decays is $^{57}\text{Co} \rightarrow {}^{57}\text{Fe}^* + e^-$, with a half-life of 271 days, followed by $^{57}\text{Fe}^* \rightarrow {}^{57}\text{Fe} + \gamma$, with a half-life of 99.3 ns. The energy of the gamma ray used in Mössbauer spectroscopy is 14.41 keV, although there are two others emitted at 123 and 137 keV. Other useful emitters are ^{119}Sn, ^{121}Sb, ^{125}Te, ^{129}I, ^{151}Eu, ^{190}Os, and ^{197}Au.

Gamma decay often involves a change in the nuclear spin. Due to the hyperfine interaction there may be several possible values for $\hbar\omega$.

Next consider the nucleus embedded in a crystal, which will be called the *source crystal*. In the discussion of the Debye–Waller factor, $\exp(-2W)$, the factor was interpreted as the probability for the crystal to be found in a periodic arrangement. If the

crystal is periodic, when one atom moves, all atoms must move. Energy conservation requires $E = \hbar\omega + (\hbar\omega)^2/2NMc^2$, where N is the number of atoms in the crystal. For a macroscopic sample the second term is negligible and so it is safe to write $E = \hbar\omega$.

Suppose that an attempt is made to absorb the gamma ray using a second crystal. The absorption process is one in which the inverse process takes place (i.e., $F + \hbar\omega \rightarrow I$). In general, this too will involve nucleus I recoiling upon absorption, and even if $E = \hbar\omega$, it would not have sufficient energy to cause the transition. However, recoilless absorption is also possible. The probability for this is given by a Debye–Waller factor for the absorbing crystal. The conclusion is that it is possible to have resonant energy transfer from one crystal to the other. This is the Mössbauer effect.

By moving one crystal relative to the other, the gamma rays are Doppler shifted. This may drive the crystals out of resonance again. Thus, if the absorber is moved toward the source at velocity v, it sees a gamma ray at frequency $\omega' = \omega[(1 + v/c)/(1 - v/c)]^{1/2} \approx \omega(1 + v/c)$. By gradually increasing v and monitoring the transmitted gamma rays through the absorbing crystal, it is possible to carefully map out the line shape of the gamma ray and hyperfine structure of the nucleus.

The utility of the Mössbauer effect is that the line shape and hyperfine splittings provide information concerning the local electronic environment of the nucleus. One compares the energy levels in the source with those of the absorber. Each is subject to a chemical shift (also called an *isomer shift*) determined, for example, by its oxidation state. The Mössbauer spectrum also provides information about the magnetic fields and spins in the solid. Thus information is provided in a similar fashion to that obtained from NMR or NQR studies. For example, one may obtain the quadrupole splitting, as in NQR. In the case of ^{57}Fe, with $I = \frac{3}{2}$, the quadrupole splitting is given by the formula $\Delta E = (e^2qQ/2)\sqrt{1 + \eta^2/3}$ [see Eq. (W22.207)]. From a measurement of the Zeeman splitting, one may determine the strength of the magnetic induction, B, at the nucleus.

An example of a Mössbauer spectrum is presented in Fig. W22.56. The gamma-ray source is $Mg_3^{125}Te^mO_6$ (with a 58-day half-life) and the absorber is ZnTe. The recoilless fraction depends on the Debye–Waller factor, $\exp[-2W(T)]$. Equation (W5.13)

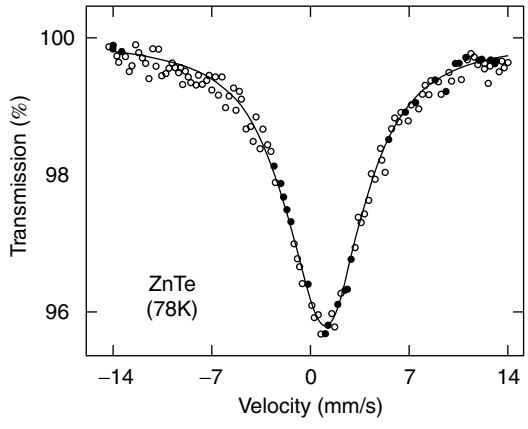

Figure W22.56. Mössbauer spectrum produced with the metastable source $Mg_3^{125}Te^m$-O_6 and the absorber ZnTe at $T = 78$ K. [From W. Bresser et al, *Phys. Rev. B*, **47**, 11663 (1993). Copyright 1993 by the American Physical Society.]

gives an expression for $W(T)$ which may be evaluated using the Debye theory used to calculate the specific heat of solids. Thus W will also depend parametrically on the Debye temperature Θ_D. By studying the Mössbauer signal as a function of temperature, it is possible to determine Θ_D. A value $\Theta_D = 188$ K is found for the absorber.

ELEMENTARY PARTICLES

The final sections of the characterization chapter are concerned with two techniques that rely on elementary particles other than the familiar ones of ordinary matter. They are positron-annihilation spectroscopy and muon-precession spectroscopy.

W22.34 Positron-Annihilation Spectroscopy

The positron is the antiparticle of the electron, with the same mass and spin but opposite charge and magnetic moment (relative to the spin). When positrons come together with electrons, pair annihilation occurs. If the pair is in a spin-singlet state and is at rest, two 0.511-MeV gamma rays are emitted in opposite directions. If the pair is in a triplet state, three gamma rays are emitted, the sum of the energies adding up to the total rest energy of 1.022 MeV. The rate for singlet decay is much faster than for triplet decay.

In positron-annihilation spectroscopy (PAS) a beam of positrons is directed at a solid and the resulting gamma-ray distribution is analyzed. Three popular ways of analyzing the data are to:

1. Measure the time decay of the gamma-ray signal
2. Measure the angular correlation of the gamma rays
3. Measure the energy distribution of the gamma rays

Typical positron sources include ^{22}Na ($\tau_{1/2} = 2.6$ years, $E = 0.54$ MeV) and ^{68}Ge ($\tau_{1/2} = 280$ days, $E = 1.89$ MeV), where E is the energy of the positron. Accelerators are also often used. The positrons are rapidly thermalized after entering the solid by making frequent collisions with the electrons and sharing their energy and momentum with them. The thermalization time is typically 25 ps. The penetration "depth" with 1% survival against annihilation is $\rho d = 10$ kg/m^2 for a 2-MeV positron, which translates into approximately 0.003 m for Al, where $\rho = 2700$ kg/m^3. A typical positron lifetime in a metal (Mg) is 232 ps.

Positrons, being positively charged, avoid the regions of high positive potential inside an atom and thus tend to settle as far from the nuclei as possible. If open-volume defects such as voids or vacancies are present, the emitted positrons are likely to settle there. Trapping can also occur in dislocations. PAS therefore provides a powerful method for studying these defects in a crystal. The decay rate per unit volume is proportional to the probability that both the electron and positron are to be found in that volume. If the positron is in a vacancy instead of being inside a normal region of the crystal, this joint probability can be expected to be lower than its normal value and hence the decay rate will also be different. The decay of the gamma-ray signal in time will also be modified. This effect may be modeled by simple kinetic equations, as follows.

Let n_f be the number of free positrons per unit volume and n_t be the corresponding number of trapped positrons per unit volume. Let the decay rate for a free positron be Γ_f and for a trapped positron be Γ_t. Let C be the concentration of traps, σ_t the trapping cross section, and v the positron speed. The rate of change of the free-positron density is given by

$$\frac{dn_f}{dt} = -\Gamma_f n_f - C\sigma_t v n_f. \tag{W22.212}$$

The rate of change of the trapped-positron density is

$$\frac{dn_t}{dt} = C\sigma_t v n_f - \Gamma_t n_t. \tag{W22.213}$$

Begin by injecting a pulse of free positrons at time $t = 0$, so

$$n_f(0) = n_0, \qquad n_t(0) = 0. \tag{W22.214}$$

The kinetic equations are readily integrated to give

$$n_f(t) = n_0 \exp[-(\Gamma_f + C\sigma_t v)t], \tag{W22.215}$$

$$n_t(t) = \frac{c\sigma_t v n_0}{\Gamma_f - \Gamma_t + c\sigma_t v}\{\exp(-\Gamma_t t) - \exp[-(\Gamma_f + c\sigma_t v)t]\}. \tag{W22.216}$$

The rate of gamma-ray production per unit volume is

$$\begin{aligned}\frac{dn_\gamma}{dt} &= n_t\Gamma_t + n_f\Gamma_f \\ &= n_0\frac{(\Gamma_f - \Gamma_t)(\Gamma_f + C\sigma_t v)}{\Gamma_f - \Gamma_t + C\sigma_t v}\exp[-(\Gamma_f + Cv\sigma_t)t] \\ &\quad + n_0\frac{C\sigma_t v\Gamma_t}{\Gamma_f - \Gamma_t + C\sigma_t v}\exp(-\Gamma_t t).\end{aligned} \tag{W22.217}$$

The exponents and amplitudes multiplying the exponentials may be extracted by fitting the time-resolved gamma-ray decay rate to a two-exponential fit.

PAS may be used to obtain information about the distribution of electrons in momentum space. In a metal the electrons fill the Fermi sea and therefore have a momentum distribution whose maximum value is determined by the Fermi energy and the band structure. The wavefunction of the electron at the location of the positron may be expanded in momentum eigenstates. The square of the expansion coefficient gives the probability of finding the electron with that momentum at the positron. The physics follows from elementary conservation laws.

Let the momentum of the electron be $\mathbf{p}$, the wave vectors of the gamma rays be $\mathbf{k}_1$ and $\mathbf{k}_2$, and the momentum of the thermalized positron be approximated by 0. Momentum conservation gives

$$\hbar[\mathbf{k}_1 + \mathbf{k}_2] = \mathbf{p}. \tag{W22.218}$$

Energy conservation gives

$$mc^2 + E = mc^2 + \sqrt{m^2c^4 + c^2p^2} = \hbar(\omega_1 + \omega_2), \tag{W22.219}$$

where E is the energy of the electron. The gamma-ray dispersion formulas are essentially those in vacuum,

$$\omega_1 = k_1 c, \qquad \omega_2 = k_2 c. \tag{W22.220}$$

Eliminating ω_1 and ω_2 leads to

$$\hbar(k_1 + k_2) = mc + \sqrt{p^2 + (mc)^2}, \tag{W22.221}$$

$$\hbar^2(k_1^2 + k_2^2 + 2k_1 k_2 \cos\theta) = p^2. \tag{W22.222}$$

where θ is the angle between $\mathbf{k}_1$ and $\mathbf{k}_2$. Solving for k_1 yields

$$\hbar k_1 = \frac{1}{2c}\left| mc^2 + E \pm \sqrt{(mc^2 + E)\left(E + mc^2 - \frac{4mc^2}{1 - \cos\theta}\right)}\right|. \tag{W22.223}$$

For the solution to be real, this formula must have a nonnegative argument for the square root. This implies that

$$1 - \cos\theta \geq \frac{4}{1 + \sqrt{1 + (p/mc)^2}}. \tag{W22.224}$$

Let $\theta = \pi - \delta$ and assume that δ is small. Then this becomes

$$-\frac{p}{mc} \leq \delta \leq \frac{p}{mc}. \tag{W22.225}$$

If there is a distribution in p values this equation implies that there will be a distribution in values of δ or, equivalently, of θ. The momentum distribution of the electrons in the solid may therefore be probed by measuring the angular-correlation function of the gamma rays.

Another way to measure the momentum distribution is to keep θ fixed at π and to measure the energy distribution of the gamma rays. Thus

$$\hbar k_1 = \frac{1}{2}\left(mc + \frac{E}{c} \pm p\right). \tag{W22.226}$$

Taking the nonrelativistic limit gives

$$\hbar\omega_1 = mc^2 \pm \frac{pc}{2}, \tag{W22.227}$$

which shows that a momentum value determines two values for the energy. The distribution of gamma-ray energies may be mapped into a distribution of electron momenta.

Thermalized positrons are emitted from the surfaces of metals as a result of the negative work functions presented by these metals to positrons, W_+. Some examples are $W_+ = -0.16$ eV for Al(100); $W_+ = -3.0$ eV for W(100) and W(110); $W_+ = -0.14$ eV for Cu(110); $W_+ = -0.33$ eV for Cu (111); and $W_+ = -1.3$ eV for Ni(100). The origin of these negative work functions is largely due to the surface

dipole layer that exists near the surfaces of metals. The positrons that are able to diffuse close to the surface are ejected with a distribution of kinetic energies centered around the negative of the work function. The width of the distribution is determined by the temperature of the solid. The angular distribution of the emitted positrons is sharply peaked around the surface normal when the surface is atomically flat and clean. For example, the full width at half maximum for W(100) positrons is $\approx 30^\circ$. Adsorbates on the surface broaden the emission cone. The emitted positrons may also display inelastic energy-loss peaks due to the excitation of surface adsorbates, much as is seen in LEELS experiments involving electrons.

Trapping of positrons by vacancies alters their decay rate, and this can be used to probe the thermal formation of vacancies in the interior of a solid. Positrons have also found use in studying multilayer interfaces and in depth profiling.

In addition to positron emission it is also possible for positronium (Ps) to be emitted. Positronium is a hydrogenic system consisting of a bound electron and positron. The binding energy of the ground state is 6.8 eV. The presence of surface defects, such as steps or vacancies, alters the emission rate for Ps.

Figure W22.57 gives an example of the electron momentum distribution obtained from the angular correlation of annihilation radiation of positrons in Cu (lower curve).

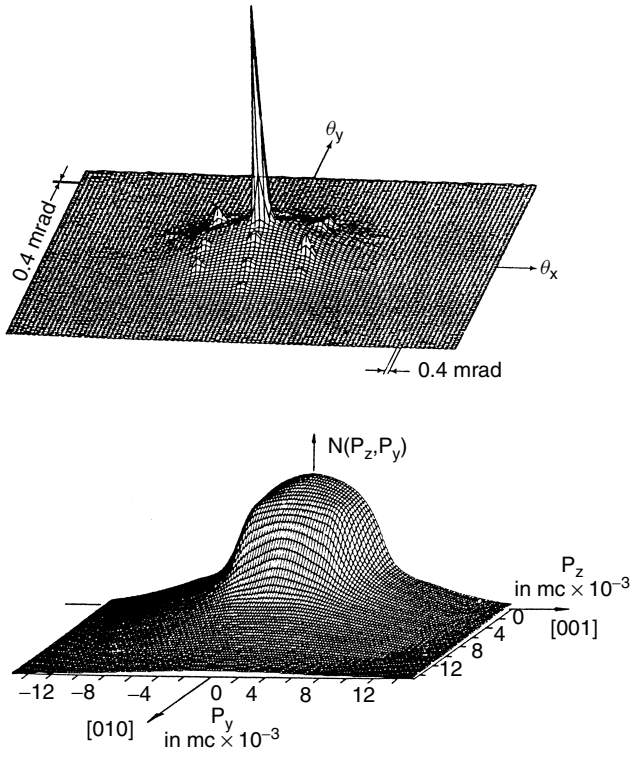

Figure W22.57. Momentum distribution of electrons obtained from studying the angular correlation of annihilation of positrons in Cu (lower curve) and the annihilation of *para*-Ps in single-crystal quartz (upper curve). [From P. J. Schultz and K. G. Lynn, *Rev. Mod. Phys.*, **60**, 701 (1988). Copyright 1988 by the American Physical Society.]

Also shown is the electron momentum distribution in single-crystal quartz (upper curve) obtained from the angular correlation of gamma rays from *para*-Ps. In Cu there is a high Fermi energy, so there is a broad distribution of electron momenta. The momentum distribution provides direct information concerning the wavefunction of the electrons in solids.

W22.35 Muon-Precession Spectroscopy

Muon precession spectroscopy (μPS) permits one to measure the spatial inhomogeneity of the magnetic field inside a material. Muons are created in an accelerator by colliding energetic particles with nuclei. At first π^+ mesons are produced, but these decay into μ^+ mesons (muons) and ν_μ neutrinos. The muons are created in a state of negative helicity (i.e., their spins point opposite to their momenta). In one type of experiment the muons enter the sample perpendicular to an external magnetic field. The implantation energy is typically 50 MeV. They rapidly slow down to an energy of 2 to 3 keV in approximately 0.1 to 1 ns. At this point they capture an electron from the material and form muonium. Muonium has the same properties as hydrogen, except the muon replaces the proton. The muonium is rapidly deexcited, on a time scale of 0.5 ps, achieving a kinetic energy of 15 eV. In another picosecond it thermalizes. Despite the fact that the muon has undergone all this deceleration and capture, the spin direction of the muon remains unchanged. The mean lifetime of the muon against decay, $\tau = 2.22$ μs, is long compared to the processes above.

The muons precess around the direction of the magnetic induction vector $\mathbf{B}_0$ at a frequency

$$\Omega(\mathbf{r}) = \frac{\mu_B B_0(\mathbf{r})}{\hbar} \frac{m_e}{m_\mu} g_\mu. \tag{W22.228}$$

Here μ_B is the Bohr magneton, m_μ the muon mass, and the g factor for the muon is $g_\mu \approx 2$. The local precession angle is $\Omega(\mathbf{r})t$. When the muon finally does decay by the process

$$\mu^+ \longrightarrow e^+ + \overline{\nu_\mu} + \nu_e, \tag{W22.229}$$

the positron e^+ is emitted preferentially along the direction of the muon-spin vector (consistent with the nonconservation of parity). The fraction of muons that live to time t is $\exp(-t/\tau)$. The product positrons are detected with sufficient angular resolution to determine the direction in which the muon spin was pointing at the time of its decay. The positron signal varies with angle and time as

$$S(\theta, t) = N_0 \exp\left(-\frac{t}{\tau}\right)[1 + A\cos(\Omega t - \theta)]. \tag{W22.230}$$

The penetration depth of the muons is large compared with the sample size, D, so only a small fraction of the muons are actually captured, but they populate the sample uniformly.

If there is a distribution of magnetic fields inside the material, there will be a distribution of precession frequencies and the angular distribution of the signal will become dephased. The time over which this occurs is a measure of the spatial inhomogeneity of the magnetic field.

Muon precession has been used to determine the local magnetic fields in antiferromagnetic materials and in ferromagnetic transition metals. It has also provided information concerning the penetration depth of magnetic fields into superconductors.

Appendix W22A: Quantum-Mechanical Description of NMR

In the development of the quantum theory of NMR in this section, the scope is limited to the case of a nucleus with spin $I = \frac{1}{2}$. Choose the quantization axis along the direction of the dc magnetic field and define it as the z direction. There are two states for the system, spin up and spin down. The time-dependent Schrödinger equation is

$$H\psi = i\hbar\frac{\partial\psi}{\partial t}, \tag{W22A.1}$$

where H is the Hamiltonian governing the system and ψ is a two-component vector with time-dependent components:

$$\psi(t) = \begin{bmatrix} u(t) \\ v(t) \end{bmatrix}. \tag{W22A.2}$$

The components $u(t)$ and $v(t)$ give the amplitudes for being in the spin-up and spin-down states, respectively. Introduce a two-dimensional matrix called the *density matrix* ρ, defined by

$$\rho = \langle\psi\psi^{+}\rangle, \tag{W22A.3}$$

where ψ^{+} is a row vector whose elements are the complex conjugates $u^{*}(t)$ and $v^{*}(t)$. The average is taken over an ensemble of ways of preparing the same state, but with different phases. Note that the density matrix is described by a Hermitian matrix (i.e., $\rho = \rho^{+}$). Also, the sum of the diagonal matrix elements of ρ (the *trace*, abbreviated $\mathrm{Tr}\rho$) is 1, since $|u|^2 + |v|^2 = 1$. It may be expanded in terms of the Pauli spin matrices, which form a basis for expanding an arbitrary 2×2 Hermitian matrix:

$$\rho = \tfrac{1}{2}[I_2 + P_x(t)\sigma_x + P_y(t)\sigma_y + P_z(t)\sigma_z] = \tfrac{1}{2}[I_2 + \boldsymbol{\sigma}\cdot\mathbf{P}(t)], \tag{W22A.4}$$

where $\mathbf{P}(t)$ is a real polarization vector and where the matrices are

$$I_2 = \begin{bmatrix} 1 & 0 \\ 0 & 1 \end{bmatrix}, \quad \sigma_x = \begin{bmatrix} 0, & 1 \\ 1 & 0 \end{bmatrix}, \quad \sigma_y = \begin{bmatrix} 0 & -i \\ i & 0 \end{bmatrix}, \quad \sigma_z = \begin{bmatrix} 1 & 0 \\ 0 & -1 \end{bmatrix}. \tag{W22A.5}$$

This form for ρ is manifestly Hermitian and obeys the trace condition $\mathrm{Tr}\rho = 1$. It follows from the Schrödinger equation that the density matrix obeys the equation

$$H\rho - \rho H = [H, \rho] = -i\hbar\frac{\partial\rho}{\partial t}. \tag{W22A.6}$$

The square bracket in this equation is called the *commutator*.

In a uniform magnetic field the Hamiltonian consists of the magnetic interaction of the dipole with the magnetic field, that is, the Zeeman interaction

$$H_0 = -\mathbf{m} \cdot \mathbf{B} = -\frac{\gamma}{2} B\sigma_Z = -\frac{\hbar}{2}\Omega\sigma_z. \tag{W22A.7}$$

There are two eigenfunctions of the time-independent Schrödinger equation $H_0\psi = E\psi$:

$$\psi_- = \begin{bmatrix} 1 \\ 0 \end{bmatrix}, \qquad \psi = \begin{bmatrix} 0 \\ 1 \end{bmatrix}, \tag{W22A.8}$$

with the corresponding eigenvalues

$$E_- = -\frac{\hbar\Omega}{2}, \qquad E = +\frac{\hbar\Omega}{2}, \tag{W22A.9}$$

where $\Omega = \gamma B/\hbar$. Suppose that the system is in thermal equilibrium at some temperature T. The Boltzmann probability for occupying the states with energy E_+ and E_- are

$$P_+ = \frac{\exp(-\beta E_+)}{\exp(-\beta E_+) + \exp(-\beta E_-)}, \quad P_- = \frac{\exp(-\beta E_-)}{\exp(-\beta E_+) + \exp(-\beta E_-)}, \tag{W22A.10}$$

where $\beta = 1/k_B T$. The density matrix corresponding to this thermal distribution is

$$\rho^0 = \frac{\exp(-\beta H_0)}{\mathrm{Tr}[\exp(-\beta H_0)]}. \tag{W22A.11}$$

In terms of the polarization vector introduced in Eq. (W22A.4), the components are

$$P_z^0 = \tanh\frac{\beta\hbar\Omega}{2}, \qquad P_x^0 = 0, \quad P_y^0 = 0. \tag{W22A.12}$$

Next introduce the rotating RF magnetic field B', as before. The Hamiltonian is

$$H = -\boldsymbol{\mu} \cdot [\mathbf{B} + \mathbf{B}'(t)] = -\frac{\hbar}{2}\Omega\sigma_z - \frac{\hbar}{2}\Omega'(\sigma_x \cos\omega t - \sigma_y \sin\omega t), \tag{W22A.13}$$

where $\Omega' = \gamma B'/\hbar$. Inserting this into the time-dependent Schrödinger equation leads to the following three equations:

$$i\dot{P}_z = -\frac{\Omega'}{2}[P_+ \exp(i\omega t) - P_- \exp(-i\omega t)], \tag{W22A.14a}$$

$$i\dot{P}_- = -\Omega P_- + \Omega' P_z \exp(i\omega t), \tag{W22A.14b}$$

$$i\dot{P}_+ = \Omega P_+ - \Omega' P_z \exp(-i\omega t), \tag{W22A.14c}$$

where

$$P_+ = P_x + iP_y, \qquad P_- = P_x - iP_y. \tag{W22A.15}$$

Next include the interaction with the other atoms of the system. The diagonal components of the density matrix represent the probabilities for being in the upper or lower state. These are taken to relax to the thermal values with a time constant called T_1. In place of Eq. (W22A.14*a*) is

$$\dot{P}_z + \frac{P_z - P_z^0}{T_1} = i\frac{\Omega'}{2}[P_+ \exp(i\omega t) - P_- \exp(-i\omega t)]. \tag{W22A.16}$$

The x and y components of the density matrix represent what are called *coherence terms*. These will also relax from their nonequilibrium values with a time constant called the *dephasing time*, T_2. Thus the following generalizations of Eqs. (W22A.14*b*) and (W22A.14*c*), including relaxation, are

$$\dot{P}_- + \frac{P_-}{T_2} = i\Omega P_- - i\Omega' P_z \exp(i\omega t), \tag{W22A.17a}$$

$$\dot{P}_+ + \frac{P_+}{T_2} = -i\Omega P_+ + i\Omega' P_z \exp(-i\omega t). \tag{W22A.17b}$$

These three formulas are called the *Bloch equations*. They are similar in form to the classical equations derived earlier [see Eqs. (W22.181) and (W22.182)]. To find a steady-state solution, let

$$P_+ = F_+ \exp(-i\omega t), \qquad P_- = F_- \exp(i\omega t) \tag{W22A.18}$$

and obtain

$$F_+ = \frac{\Omega' P_z}{\Omega - \omega - i/T_2}, \qquad F_- = \frac{\Omega' P_z}{\Omega - \omega + i/T_2}, \tag{W22A.19}$$

where

$$P_z = P_z^0 \frac{(\Omega - \omega)^2 T_2^2 + 1}{(\Omega - \omega)^2 T_2^2 + (1 + T_1 T_2 \Omega'^2)}. \tag{W22A.20}$$

This expression demonstrates that the probability of finding the system in the upper-energy state is increased above that expected at thermal equilibrium. The probability of finding the system in the lower-energy state is decreased correspondingly. The maximum increase occurs at resonance, when $\omega = \Omega$. The full-width at half maximum of the resonance is

$$\Delta\omega = \frac{2}{T_2}\sqrt{1 + T_1 T_2 \Omega'^2}. \tag{W22A.21}$$

By studying the behavior of $\Delta\omega$ as a function of Ω' it is possible to extract the parameters T_1 and T_2.

Since the populations of atoms in the upper and lower energy levels change as the RF frequency is varied, the magnetic energy of nuclei must also change. This energy must have come from somewhere. Since a dc magnetic field is incapable of supplying energy, it must have come from the RF field. The RF oscillator supplying the RF field experiences an added resistive and inductive component in the resonant circuit. This

may be monitored electronically, and the location of the resonance frequency may be determined.

REFERENCES

General

Brundle, C. R., C. A. Evans, Jr., and S. Wilson, eds., *Encyclopedia of Materials Characterization*, Butterworth-Heinemann, Boston, 1992.

Bulletin of the Materials Research Society.

Kane, P. F., and G. B. Larrabee, eds., *Characterization of Solid Surfaces*, Plenum Press, New York, 1974.

Wachtman, J. B., *Characterization of Materials*, Butterworth-Heinemann, Boston, 1993.

X-ray Diffraction

Cullity, B. D., *Elements of X-ray Diffraction*, 2nd ed., Addison-Wesley, Reading, Mass., 1978.

Suryanarayana, C., and M. B. Norton, *X-ray Diffraction: A Practical Approach*, Plenum Press, New York, 1998.

Zachariasen, W. H., *Theory of X-ray Diffraction in Crystals*, Wiley, New York, 1945.

LEED

Brundle, C. R., *Electron Spectroscopy: Theory, Techniques and Applications*, Academic Press, San Diego. Calif., 1977.

Pendry, J. B., *Low Energy Electron Diffraction: The Theory and Its Application to Determination of Surface Structure*, Academic Press, San Diego, Calif., 1974.

Sevier, K. D., *Low Energy Electron Spectrometry*, Wiley-Interscience, New York, 1972.

van Hove, M. A., W. H. Weinberg, and C. M. Chan, *Low-Energy Electron Diffraction: Experiment, Theory, and Surface Structure Determination*, Springer-Verlag, Berlin, 1986.

RHEED

Larsen, P. K., and P. J. Dobson, eds., *Reflection High-Energy Electron Diffraction and Reflection Electron Imaging of Surfaces*, Plenum Press, New York, 1988.

Neutron Scattering

Ashcroft, N. W., and N. D. Mermin, *Solid State Physics*, Saunders College, Philadelphia, 1976.

Bacon, G. E., *Neutron Diffraction*, 3rd ed., Clarendon Press, Oxford, 1980.

Optical Spectroscopy

Palik, E. D., ed., *Handbook of Optical Constants of Solids*, Academic Press, San Diego, Calif., Vol. 1: 1985, Vol. II: 1991.

Ellipsometry

Aspnes, D. E., The accurate determination of optical properties by ellipsometry, in, E. D. Palik, ed., *Handbook of Optical Constants of Solids* Vol. I, Academic Press, San Diego, Calif., 1985.

Azzam, R. M. A., Ellipsometry, in, M. Bass, ed., *Handbook of Optics*, Vol. 2, McGraw-Hill, New York, 1995.

Jackson, J. D., *Electrodynamics*, 2nd ed., Wiley, New York, 1975.

FTIR

Bell, R. J., *Introductory Fourier Transform Spectroscopy*, Academic Press, San Diego, Calif., 1972.

Chamberlain, J. E., *The Principles of Interferometric Spectroscopy*, Wiley, New York, 1979.

Griffiths, P. R., and J. H. de Haseth, *Fourier Transform Infrared Spectrometry*, Wiley, New York, 1986.

Raman Scattering

Colthup, N. B., *Introduction to Infrared and Raman Spectroscopy*, 3rd ed., Academic Press, San Diego, Calif., 1990.

Ferraro, J. R., *Introductory Raman Spectroscopy*, Academic Press, San Diego, Calif., 1994.

Herzberg, G., Molecular spectra and molecular structure, in *Infrared and Raman Spectra of Polyatomic Molecules*, Prentice-Hall, New York, 1939.

Ferraro, J. R., and K. Nakamoto, eds., *Introductory Raman Spectroscopy*, Academic Press, San Diego, Calif., 1994.

Luminescence

Alfano, R. R., *Semiconductors Probed by Ultrafast Laser Spectroscopy*, Academic Press, San Diego, Calif., 1984.

Ropp, R. C., Luminescence and the Solid State, Vol. 12 of *Studies in Inorganic Chemistry*, Elsevier, Amsterdam, 1991.

Nonlinear Spectroscopy

Bloembergen, N., *Nonlinear Optics*, Addison-Wesley, Reading, Mass., 1992.

Butcher, N., and D. Cotter, *The Elements of Nonlinear Optics*, Cambridge University Press, New York, 1990.

Mills, D. L., *Nonlinear Optics: Basic Concepts*, Springer-Verlag, New York, 1991.

Newell, A. C., and J. V. Moloney, *Nonlinear Optics*, Addison-Wesley, Reading, Mass., 1992.

Shen, Y. R., *The Principles of Nonlinear Optics*, Wiley, New York, 1984.

SEM

Goldstein, J. I., et al, *Scanning Electron Microscopy and X-ray Microanalysis: A Text for Biologists, Materials Scientists, and Geologists*, 2nd ed., Plenum Press, New York, 1992.

Lyman, C. E., et al., *Scanning Electron Microscopy, X-ray Microanalysis and Analytical Electron Microscoscopy*, Plenum Press, New York, 1990.

Reimer, L., in P. Hawkes, ed., *Scanning Electron Microscope*, Springer-Verlag, Berlin, 1985.

TEM

Edington, J. W., *Practical Electron Microscopy in Materials Science*, N. V. Philips, Eindhoven, The Netherlands, 1976.

Reimer, L., *Transmission Electron Microscopy*, Springer-Verlag, Berlin, 1984.

HRTEM

Buseck, P., J. Cowley, and L. Eyring, eds., *High-Resolution Transmission Electron Microscopy and Associated Techniques*, Oxford University Press, New York, 1988.

Spence, J. C. H., *Experimental High Resolution Electron Microscopy*, Oxford University Press, New York, 1988.

LEEM

Howie, A., and U. Valdre, eds., *Study of Surfaces and Interfaces by Electron Optical Techniques*, Plenum Press, New York, 1987.

Photoemission

Cardona, M., and L. Ley, eds., *Photoemission in Solids*, Springer-Verlag, Berlin, 1978.

Feuerbacher, B., ed., *Photoemission and the Electronic Properties of Surfaces*, Wiley, New York, 1978.

XPS

Carlson, T. A., *Photoelectron and Auger Spectroscopy*, Plenum Press, New York, 1978.

Ibach, H., ed., *Electron Spectroscopy for Chemical Analysis*, ed., Springer-Verlag, Berlin, 1978.

LEELS

Ibach, H., *Electron Energy Loss Spectroscopy and Surface Vibrations*, Academic Press, San Diego, Calif., 1982.

EXAFS

Koningsberger, D. C., and R. Prins, eds., *X-ray Absorption: Principles, Applications, Techniques of EXAFS, SEXAFS, and XANES*, Wiley, New York, 1988.

Teo, B. K., *EXAFS: Basic Principles and Data Analysis*, Springer-Verlag, Berlin, 1986.

AES

Briggs, D., and M. P. Seah, *Practical Surface Analysis by Auger and X-ray Photoelectron Spectroscopy*, Wiley, New York, 1983.

SIMS

Benninghoven, A., F. G. Rudenauer, and H. W. Werner, *Secondary Ion Mass Spectroscopy*, Wiley-Interscience, New York, 1987.

RBS

Chu, W. K., J. W. Mayer, and M. A. Nicolet, *Backscattering Spectrometry*, Academic Press, San Diego, Calif., 1978.

Feldman, L. C., and J. W. Mayer, *Fundamentals of Surface and Thin Film Analysis*, North-Holland, New York, 1986.

AFM

Sarid, D., *Scanning Force Microscopy with Applications to Electric, Magnetic and Atomic Forces*, Oxford University Press, New York, 1991.

STM

Neddermeyer, H. ed., *Scanning Tunneling Microscopy*, Vol. 6, *Perspectives in Condensed Matter Physics*, Kluwer, Boston, 1993.

Transport Measurements

Lark-Horovitz, K., and V. A. Johnson, eds., *Solid State Physics*, in Marton, L. ed., *Methods of Experimental Physics*, Vol. 6, Academic Press, San Diego, Calif., 1959.

NMR and NQR

Abragam, A., *The Principles of Nuclear Magnetism*, Oxford University Press, Oxford, 1978.

Slichter, C. P., *Principles of Magnetic Resonance*, 3rd enlarged and updated ed. Springer-Verlag, Berlin, 1990.

ESR

Abragam, A., and B. Bleaney, *Electron Paramagnetic Resonance of Transition Ions*, Clarendon Press, Oxford, 1970.

Pake, G. E., *Paramagnetic Resonance*, W.A. Benjamin, New York, 1962.

Poole, C. P., and H. A. Farach, *Theory of Magnetic Resonance*, 2nd ed., Wiley, New York, 1987.

Mössbauer Effect

Gibb, T. C., *Principles of Mössbauer Spectroscopy*, Chapman & Hall, London, 1976.

Wertheim, G. K., *Mössbauer Effect: Principles and Applications*, Academic Press, San Diego, Calif., 1964.

PAS

Coleman, C. F., and A. E. Hughes, Positron annihilation, in *Research Techniques in Nondestructive Testing*, Vol. 3, R. S. Sharpe, ed., Academic Press, San Diego, Calif., 1977.

Hautojarui, P., *Positrons in Solids*, Springer-Verlag, Berlin, 1979.

μPS

Chappert, J., and R. I. Grynczpan, eds., *Muons and Pions in Materials Research*, North-Holland, Amsterdam, 1984.

PROBLEMS

W22.1 A beam of x-rays impinges on the surface of a metal at a small angle of incidence. Treat the metal as a plasma. Show that total-internal reflection is possible when the angle is sufficiently small. Derive an expression for the critical angle in terms of the plasma frequency of the metal and the frequency of the x-rays.

W22.2 The Bragg description of x-ray scattering assumes that specular scattering from the various lattice planes occurs. What happens when nonspecular scattering occurs? Does one find additional peaks due to nonspecular scattering?

W22.3 Light is incident normally on a film of material of thickness D characterized by the complex index of refraction $\tilde{n} = n + i\kappa$. Derive expressions for the reflection coefficient and the transmission coefficient. What fraction of the radiation is absorbed inside the medium? Consider the multiple reflections inside the slab.

W22.4 Given the dielectric function $\epsilon(\omega) = 1 - \omega_p^2/\omega(\omega + i/\tau)$ for a plasma, verify the following sum rules:

$$\int_0^\infty \omega\epsilon_2(\omega)d\omega = \frac{\pi}{2}\omega_p^2,$$

$$\int_0^\infty [n(\omega) - 1]d\omega = 0,$$

$$\epsilon_1(\omega) = \frac{2}{\pi}\mathscr{P}\int_0^\infty \frac{\omega'\epsilon_2(\omega')}{\omega'^2 - \omega^2}d\omega',$$

$$\epsilon_2(\omega) - \frac{4\pi}{\omega}\sigma(0) = -\frac{2}{\pi}\omega\mathscr{P}\int_0^\infty \frac{\epsilon_1(\omega') - 1}{\omega'^2 - \omega^2}d\omega'.$$

[The symbol $\mathscr{P}$ denotes taking the "principal part" (i.e., leaving out a small region around the singularity when evaluating the integral and then making the region smaller and smaller in such a way that the integral remains nonsingular).] The last two equations are called the *Kramers–Kronig relations*. All these formulas are general.

W22.5 Derive the Rutherford differential scattering cross section for a charge Z_1e, moving with kinetic energy E, scattering through an angle θ off a stationary charge Z_2e:

$$\frac{d\sigma}{d\Omega} = \frac{Z_1^2Z_2^2e^4}{16E^2(4\pi\epsilon_0)^2}\frac{1}{\sin^4(\theta/2)}.$$

W22.6 Derive the cross section for an ion of charge Ze scattering from a molecule and vibrationally exciting it. To a first approximation, assume that the charge

moves on a straight line with velocity v and impact parameter b. Model the molecule as a simple harmonic oscillator with spring constant k, mass M, and a charge $+q$ at one end of the spring and $-q$ at the other end. Compute the impulse delivered to the oscillator. Assume that the oscillator is excited when the energy transferred exceeds the vibrational quantum of energy hf. Proceed to calculate the cross section for low-energy electron loss spectroscopy from a layer of molecules on the surface of a solid.

W22.7 Repeat the calculation in Problem. W22.6 using the Born approximation (i.e., representing the incident and outgoing wavefunctions as plane waves and using first-order time-dependent perturbation theory). Assume that the moving charge couples to the harmonic oscillator by the Coulomb interaction. You may assume that the amplitude for molecular vibration is small compared with other relevant distances.

W22.8 In the atomic-force microscope, as well as the scanning-tunneling microscope, it is important to try to eliminate the effect of external vibrations as much as possible. Model the cantilever and stylus as a spring–mass system, with resonant frequency ω_0, as shown in Fig PW22.8. Show that if the entire microscope is made to oscillate up and down with frequency ω and amplitude A, the distance between the stylus and the sample will oscillate with the same frequency but with an amplitude approximated by $(\omega/\omega_0)^2 A$, when $\omega \ll \omega_0$.

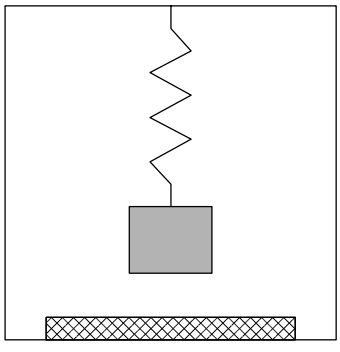

Figure PW22.8

W22.9 K-shell electrons of Cl^- ions in NaCl absorb x-rays of wavelength λ. The energy needed to ionize this electron from the K shell will be denoted by I_K. The NN distance is denoted by a. EXAFS oscillations are observed when λ is varied. Find the periods of these oscillations. Include the effect from NNs and next-NNs.

W22.10 Electrons with 200 eV energy are incident on the (100) face of GaAs. Find the angles at which the LEED beams will emerge. Repeat the calculation for the (111) and (110) faces.

W22.11 Calculate the force between the stylus of the atomic-force microscope and a solid material. Model the stylus as a sphere of radius R and the solid as a half-space filled with material in the region $z < 0$. Let the minimum distance between the sphere and plane be H. Assume a concentration n_s of atoms per

unit volume in the stylus and correspondingly n_m in the material. Assume that each stylus atom interacts with each material atom through the Lennard-Jones potential given in Eq. (2.3):

$$u(r) = 4\varepsilon \left[\left(\frac{\sigma}{r}\right)^{12} - \left(\frac{\sigma}{r}\right)^{6} \right],$$

where ε and σ are constants characterizing the interaction and the $1/r^6$ term represents the van der Waals potential. (To obtain a precise answer, it will probably be necessary to do a numerical integration. You may, instead, make whatever reasonable assumptions are necessary to obtain an estimate.)

W22.12 A silver mirror is found to have a reflectivity R as a function of wavelength λ given by the following data:

$\lambda(\mu\text{m})$	0.20	0.30	0.40	0.50	0.60	0.70	0.80	0.90	1.00
R (%)	20	12	85	91	93	95	97	98	98

Why is the reflectivity so high at long wavelengths? Use the data above to estimate the plasma frequency, ω_p, of Ag.

W22.13 An x-ray diffraction study of $(Ca_{0.3}Sr_{0.7})_{0.9}CuO_2$ made with the Cu(Kα) line ($\lambda = 0.1544$ nm) reveals peaks at the following values of the angle $\psi = 2\theta$ (in degrees): 23.1, 26.7, 32.4, 35.3, 42.6, 46.5, 54.9, 59.8, 65.4, 68.2. The crystal is believed to be orthorhombic. Find the reciprocal lattice vectors and lattice constants.

W22.14 Indium, at room temperature, is a tetragonal crystal with $a = 0.325$ nm and $c = 0.495$ nm. Find the 2θ values for the first 16 x-ray diffraction peaks. Assume that the Mo (Kα) line is used ($\lambda = 0.07136$ nm).

W22.15 Six surfaces of a crystal are shown in Fig. PW22.15. The two leftmost figures show the (100) and (111) faces of an FCC crystal. The remaining figures show adsorbed atoms on these faces. In the primitive 2×2 [$p(2 \times 2)$] structures and the centered 4×2 structure [$c(4 \times 2)$] one-fourth of a monolayer is adsorbed. In the centered 2×2 structure [$c(2 \times 2)$], one-half of a monolayer is adsorbed. Find the LEED pattern from each of the six surfaces.

(*Note*: Often, faces of pure crystals will reconstruct and substrate atoms will occupy the sites occupied by adsorbate atoms, as in this example.)

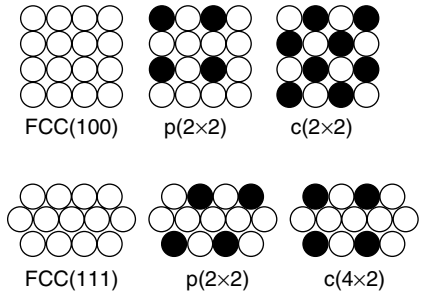

Figure PW22.15

W22.16 Ring patterns are formed when x-rays are diffracted from a crystalline powder. Show that the radii of the rings vary with the integers N as $r_N \propto \sqrt{N}$. What are the allowable values for N for the following crystal structures: simple cubic, BCC, FCC, and diamond?

W22.17 Given $\Delta\theta = 0.05$ rad for the (100) diffraction maximum from polycrystalline Al, use Eq. (W22.4) to find the average crystallite size. Use $\lambda = 0.1$ nm.

Computer Problems

W22.18 To get a feeling for the design of an electron microscope, write a program to determine the focal length for a beam of electrons directed toward a charged ring at normal incidence. To do this, obtain an expression for the electric field at an arbitrary point in space set up by a charged ring of unit radius. This may be left as an integral over the length elements of the ring. Numerically integrate Newton's second law, taking as the initial condition the displacement of the electron from the axis. Determine where this beam crosses the symmetry axis. Show that to a first approximation, this focal length is independent of the original distance from the axis. To the next approximation you may use the program to study the spherical aberrations of this electrostatic lens.

W22.19 Repeat Problem W22.18 for an electron beam directed at a circular loop of wire carrying an electric current. This time use the Biot–Savart formula to calculate the magnetic field at an arbitrary point in space, and calculate the magnetic force on a moving electron. Proceed as before to integrate Newton's equations of motion numerically.

W22.20 A commonly used device in SIMS is the electrostatic quadrupole mass analyzer. It consists of four parallel cylinders whose projections form a square. Two diagonally opposite wires are positively charged and the other two are negatively charged. Show that to a first approximation, the angle of deflection of an electron beam is independent of its distance from the plane of reflection symmetry of the wires. To the next approximation, study the aberrations of this device.

APPENDIX WA

Thermodynamics

Thermodynamic variables are classified as *extensive* if they scale as the volume of the system, V. Thus U, the internal energy, N, the number of particles, and S, the entropy, are extensive variables. (Here attention is restricted to a system in which there is only one kind of particle.) Variables that do not scale as the size of the system are called *intensive*. The internal energy of the system may be expressed as a function of the extensive variables [i.e., $U = U(V, N, S)$]. Thus

$$\begin{aligned} dU &= \left(\frac{\partial U}{\partial V}\right)_{N,S} dV + \left(\frac{\partial U}{\partial N}\right)_{V,S} dN + \left(\frac{\partial U}{\partial S}\right)_{N,V} dS \\ &= -P\,dV + \mu\,dN + T\,dS. \end{aligned} \tag{WA.1}$$

One sees by comparing the coefficients of dV, dN, and dS that P, the pressure, T, the temperature, and μ, the chemical potential, are intensive variables. Equation (WA.1) is known as the *first law of thermodynamics*. It recognizes that energy is conserved and that heat is a form of energy. The differential quantity TdS represents the heat input to a system, $P\,dV$ is the work done by the system, $-\mu\,dN$ the energy transported by particles leaving the system, and dU the increase of internal energy of the system.

Since one often has control over variables other than (V, N, S) it is convenient to introduce thermodynamic potentials. The Helmholtz free energy, F, is defined as

$$F = U - TS. \tag{WA.2}$$

Forming the differential and combining the result with Eq. (WA.1) leads to

$$dF = -P\,dV + \mu\,dN - S\,dT. \tag{WA.3}$$

The Helmholtz free energy is useful in problems in which one controls the variables (V,N,T). If (V,N,T) are constant, $dF = 0$ at equilibrium.

The enthalpy, H, is defined by

$$H = U + PV. \tag{WA.4}$$

Its differential leads to the formula

$$dH = T\,dS + \mu\,dN + V\,dP. \tag{WA.5}$$

The enthalpy is used when one controls (S,N,P). If (S,N,P) are held constant, $dH = 0$ at equilibrium.

The *Gibbs free energy* is defined by

$$G = U - TS + PV = F + PV = H - TS. \tag{WA.6}$$

Its differential results in

$$dG = \mu\, dN - S\, dT + V\, dP. \tag{WA.7}$$

The Gibbs free energy is of use in problems where one controls (N,T,P). If (N,T,P) are held constant, $dG = 0$ at equilibrium.

From Eqs. (WA.2), (WA.4), and (WA.6), one sees that F, H, and G are all extensive variables. One may integrate Eq. (WA.1) to obtain the Euler relation

$$U = -PV + \mu N + TS, \tag{WA.8}$$

from which it is seen that

$$G = N\mu. \tag{WA.9}$$

The chemical potential for a one-component system is thus the Gibbs free energy per particle. From Eqs. (WA.1) and (WA.8) one obtains the *Gibbs–Duhem formula*:

$$N\, d\mu = V\, dP - S\, dT. \tag{WA.10}$$

A number of thermodynamic relations follow from expressing Eqs. (WA.1), (WA.3), (WA.5), and (WA.7) as partial derivatives. They are

$$T = \left(\frac{\partial U}{\partial S}\right)_{N,V}, \qquad P = -\left(\frac{\partial U}{\partial V}\right)_{N,S}, \qquad \mu = \left(\frac{\partial U}{\partial N}\right)_{V,S}, \tag{WA.11a}$$

$$P = -\left(\frac{\partial F}{\partial V}\right)_{N,T}, \qquad S = -\left(\frac{\partial F}{\partial T}\right)_{N,V}, \qquad \mu = \left(\frac{\partial F}{\partial N}\right)_{V,T}, \tag{WA.11b}$$

$$T = \left(\frac{\partial H}{\partial S}\right)_{N,P}, \qquad \mu = \left(\frac{\partial H}{\partial N}\right)_{P,S}, \qquad V = \left(\frac{\partial H}{\partial P}\right)_{N,S}, \tag{WA.11c}$$

$$\mu = \left(\frac{\partial G}{\partial N}\right)_{T,P}, \qquad S = -\left(\frac{\partial G}{\partial T}\right)_{N,P}, \qquad V = \left(\frac{\partial G}{\partial P}\right)_{N,T}. \tag{WA.11d}$$

A pair of useful mathematical identities follow from forming the differential of a function $z(u,v)$:

$$dz = \left(\frac{\partial z}{\partial u}\right)_v du + \left(\frac{\partial z}{\partial v}\right)_u dv, \tag{WA.12}$$

and then forming $u(z,v)$,

$$dz = \left(\frac{\partial z}{\partial u}\right)_v \left(\left(\frac{\partial u}{\partial z}\right)_v dz + \left(\frac{\partial u}{\partial v}\right)_z dv\right) + \left(\frac{\partial z}{\partial v}\right)_u dv, \tag{WA.13}$$

Matching coefficients of like differentials leads to

$$1 = \left(\frac{\partial z}{\partial u}\right)_v \left(\frac{\partial u}{\partial z}\right)_v, \tag{WA.14}$$

$$0 = \left(\frac{\partial z}{\partial u}\right)_v \left(\frac{\partial u}{\partial v}\right)_z + \left(\frac{\partial z}{\partial v}\right)_u. \tag{WA.15}$$

The Maxwell relations are a set of formulas that state that the order of differentiation does not matter when a second derivative is formed. Thus, for $z(u,v)$,

$$dz = \left(\frac{\partial z}{\partial u}\right)_v du + \left(\frac{\partial z}{\partial v}\right)_u dv \equiv \xi\, du + \eta\, dv, \tag{WA.12$'$}$$

the Maxwell relation is

$$\left(\frac{\partial \xi}{\partial v}\right)_u = \left(\frac{\partial \eta}{\partial u}\right)_v. \tag{WA.16}$$

Applying this to Eqs. (WA.1), (WA.3), (WA.5), and (WA.7) gives

$$-\left(\frac{\partial P}{\partial N}\right)_{V,T} = \left(\frac{\partial \mu}{\partial V}\right)_{N,T}, \quad \left(\frac{\partial P}{\partial T}\right)_{V,N} = \left(\frac{\partial S}{\partial V}\right)_{N,T}, \quad \left(\frac{\partial \mu}{\partial T}\right)_{V,N} = -\left(\frac{\partial S}{\partial N}\right)_{V,T} \tag{WA.17}$$

$$-\left(\frac{\partial P}{\partial N}\right)_{V,S} = \left(\frac{\partial \mu}{\partial V}\right)_{N,S}, \quad -\left(\frac{\partial P}{\partial S}\right)_{V,N} = \left(\frac{\partial T}{\partial V}\right)_{N,S}, \quad \left(\frac{\partial \mu}{\partial S}\right)_{V,N} = \left(\frac{\partial T}{\partial N}\right)_{V,S} \tag{WA.18}$$

$$\left(\frac{\partial T}{\partial N}\right)_{S,P} = \left(\frac{\partial \mu}{\partial S}\right)_{N,P}, \quad \left(\frac{\partial T}{\partial P}\right)_{S,N} = \left(\frac{\partial V}{\partial S}\right)_{N,P}, \quad \left(\frac{\partial \mu}{\partial P}\right)_{S,N} = \left(\frac{\partial V}{\partial N}\right)_{S,P} \tag{WA.19}$$

$$\left(\frac{\partial \mu}{\partial T}\right)_{N,P} = -\left(\frac{\partial S}{\partial N}\right)_{T,P}, \quad \left(\frac{\partial \mu}{\partial P}\right)_{T,N} = \left(\frac{\partial V}{\partial N}\right)_{T,P}, \quad -\left(\frac{\partial S}{\partial P}\right)_{T,N} = \left(\frac{\partial V}{\partial T}\right)_{N,P}. \tag{WA.20}$$

The heat capacity at constant pressure and constant number of particles is

$$C_{P,N} = T\left(\frac{\partial S}{\partial T}\right)_{P,N} = \left(\frac{\partial H}{\partial T}\right)_{P,N}. \tag{WA.21a}$$

The heat capacity at constant volume and constant number is

$$C_{V,N} = T\left(\frac{\partial S}{\partial T}\right)_{V,N} = \left(\frac{\partial U}{\partial T}\right)_{V,N}. \tag{WA.21b}$$

The *second law of thermodynamics* states that the entropy of the universe (system plus environment) never decreases [i.e., $\Delta S \geq 0$]. Of course, S can decrease locally, as when a system orders, but this decrease must be matched by at least as large an increase in the entropy of the environment. An idealized process in which $\Delta S = 0$ is called a *reversible process*.

The *third law of thermodynamics* states that the entropy of a pure crystalline material is zero at $T = 0$ K. At $T = 0$ K the system finds itself in the ground state. If g is the

degeneracy of that state, $g/N \to 0$ as $N \to \infty$. The third law implies that is impossible for the system to attain the temperature $T = 0$ K.

For a multicomponent system, one generalizes Eq. (WA.1) to

$$dU = -P\,dV + \sum_i \mu_i\,dN_i + T\,dS. \tag{WA.1a}$$

One may simply regard the quantities μ_i and N_i as elements of vectors and interpret terms like $\mu\,dN$ in the previous formulas as being scalar products between these vectors.

One may apply thermodynamics to a chemically reacting system. For such a system, the set $\{N_j\}$ denotes the reactants or products. In a chemical reaction

$$\sum_j \nu_j A[j] = 0, \tag{WA.22}$$

where $A[j]$ is the symbol for chemical j (e.g., $A = \text{Cu}$ or $A = \text{SiO}_2$). The stoichiometric coefficients ν_j are positive integers for the reactants and negative integers for the products. If dM is the number of times that this reaction occurs, $dN_j = \nu_j dM$. Inserting this into Eq. (WA.7) gives, for equilibrium at constant P and T,

$$\frac{dG}{dM} = \sum_j \nu_j \mu_j = 0. \tag{WA.23}$$

This is called the *equation of reaction equilibrium* and relates the different chemical potentials of the products and reactants.

At equilibrium some extremal principles apply: For fixed (N,V,U), S will be maximized; for fixed (N,V,T), F will be minimized; for fixed (S,N,P), H will be minimized; for fixed (N,T,P), G will be minimized.

APPENDIX WB

Statistical Mechanics

Statistical mechanics provides the theoretical link between the microscopic laws of physics and the macroscopic laws of thermodynamics. Rather than attempt to solve the microscopic laws in their entirety (which is presumably very difficult), one abstracts some key concepts, such as conservation laws, and augments them with certain statistical assumptions about the behavior of systems with large numbers of particles in order to make the problem tractable.

The first goal will be to make contact with the first law of thermodynamics, $T\,dS = dU + P\,dV$, as given in Eq. (WA.1) (for constant N). Consider a system of N particles whose possible energy is E_i. One way to obtain statistical information is to create an ensemble (i.e., one replicates this system a large number of times, M, and imagines that the various systems can exchange energy with each other). Let M_i denote the number of systems with energy E_i. The total number of systems must be M, so

$$\sum_i M_i = M. \tag{WB.1}$$

Conservation of energy requires that

$$\sum_i M_i E_i = E, \tag{WB.2}$$

where E is the total energy of the ensemble.

The total number of ways in which M systems can be distributed into groups with $(M_1, M_2, \ldots)$ members in each group, respectively, is

$$W = \frac{M!}{M_1!\,M_2!\ldots}. \tag{WB.3}$$

One wishes to find the most-probable set of values for the M_i. Therefore, one looks for the set that maximizes W [or equivalently $\ln(W)$] subject to the constraints imposed by Eqs. (WB.1) and (WB.2). Thus, introducing Lagrange multipliers α and β to enforce the constraints, one has

$$\delta\left[\ln W - \alpha\left(\sum_i M_i - N\right) - \beta\left(\sum_i M_i E_i - E\right)\right] = 0. \tag{WB.4}$$

Use is made of Stirling's approximation, $\ln M! \approx M \ln M - M$ for $M \gg 1$, to write this as

$$\delta\left[M \ln M - M - \sum_i (M_i \ln M_i - M_i) - \alpha\left(\sum_i M_i - M\right) - \beta\left(\sum_i M_i E_i - E\right)\right] = 0. \tag{WB.5}$$

One may now differentiate with respect to the individual M_i and set the derivatives equal to zero. This leads to

$$M_i = e^{-\alpha - \beta E_i}. \tag{WB.6}$$

The probability of finding a particular state i in the most-likely probability distribution is given by the formula

$$p_i = \frac{M_i}{M} = \frac{e^{-\beta E_i}}{\sum_i e^{-\beta E_i}}, \tag{WB.7}$$

where, clearly, $\sum p_i = 1$. Equation (WB.7) indicates that it less probable to find high-energy states than low-energy states.

Introduce the canonical partition function for the N-particle system

$$Z_N = \sum_i e^{-\beta E_i}. \tag{WB.8}$$

The function Z_N is given by a sum of terms, each term representing the relative probability for finding the system in the state i with energy E_i. The mean entropy of a system is defined as

$$S = \frac{k_B}{M} \ln W = -k_B \sum_i p_i \ln p_i, \tag{WB.9}$$

where use has been made of Eq. (WB.7). The mean energy of the system, interpreted as the internal energy, U, is given by

$$U = \sum_i p_i E_i. \tag{WB.10}$$

Note that if a small change were made in the $\{p_i\}$, the corresponding changes in the entropy and internal energy would give rise to

$$\delta\left(U - \frac{S}{k_B \beta}\right) = \left(\sum_i E_i \delta p_i + \frac{1}{\beta} \sum_i \ln p_i \delta p_i + \frac{1}{\beta} \sum_i \delta p_i\right) \tag{WB.11}$$

since $\sum_i \delta p_i = 0$. This is consistent with the first law of thermodynamics $dU - T\,dS = -P\,dV$, when T and V (and N) are held constant. Thus one may interpret the parameter $\beta = 1/k_B T$ as being proportional to the inverse absolute temperature. The Helmholtz free energy is $F = U - TS$ and, from Eqs. (WB.7), (WB.8), and (WB.9), is simply related to the partition function

$$Z_N = e^{-\beta F}. \tag{WB.12}$$

Now consider an N-particle system of noninteracting identical particles. The individual energies for a given particle will be denoted by ϵ_i. A state of the system is defined by specifying the number of particles in each state (i.e., by a set of integers $\{n_i\}$). Thus

$$N = \sum_i n_i, \tag{WB.13}$$

$$E(n_1, n_2, \ldots) = \sum_i n_i \epsilon_i. \tag{WB.14}$$

From Eq. (WA.1) recall that the first law of thermodynamics for a system with a variable number of particles may be written as $T\,dS = dU - \mu\,dN + P\,dV$, where μ is the chemical potential. The analysis proceeds much as before, with the exception that one now will be measuring the energies of the particles relative to the chemical potential. The average number of particles in a given state is given by

$$\langle n_j \rangle = \frac{\sum_{n_1}\sum_{n_2}\cdots n_j e^{-\beta\Sigma_i(\epsilon_i-\mu)n_i}}{\sum_{n_1}\sum_{n_2}\cdots e^{-\beta\Sigma_i(\epsilon_i-\mu)n_i}} = \frac{\sum_{n_j} n_j e^{-\beta(\epsilon_j-\mu)n_j}}{\sum_{n_j} e^{-\beta(\epsilon_j-\mu)n_j}}. \tag{WB.15}$$

For particles with spin $\frac{1}{2}$, $\frac{3}{2}$, ... obeying Fermi–Dirac statistics, such as electrons (spin $\frac{1}{2}$), the only possible values for n_j are 0 or 1. This leads to the mean number of particles in a given state:

$$f(\epsilon_j, T) = \langle n_j \rangle = \frac{1}{e^{\beta(\epsilon_j-\mu)} + 1}. \tag{WB.16}$$

This is known as the *Fermi–Dirac distribution function*. For particles with spin 0, 1, 2,... obeying Bose–Einstein statistics, such as photons or phonons, any nonnegative integer is acceptable for n_j. Performing the sums in Eq. (WB.15) leads to the *Bose–Einstein distribution function*:

$$\langle n_j \rangle = \frac{1}{e^{\beta(\epsilon_j-\mu)} - 1}. \tag{WB.17}$$

In the high-temperature limit, Eqs. (WB.16) and (WB.17) both reduce to the Maxwell–Boltzmann distribution when $\epsilon_j - \mu \gg k_B T$:

$$\langle n_j \rangle \longrightarrow e^{-\beta(\epsilon_j-\mu)}. \tag{WB.18}$$

APPENDIX WC

Quantum Mechanics

In the short space of an appendix it is not possible to develop quantum mechanics. However, it is possible to review some of the key concepts that are used in the textbook[†] and at the Web site.

In the Schrödinger description of quantum mechanics a physical system such as an atom or even a photon is described by a wavefunction ψ. The wavefunction depends on the variables describing the degrees of freedom of the system and on time. Thus for a particle moving in one dimension, the wavefunction is $\psi\ (x,\ t)$; for a particle moving in three dimensions, it is $\psi\ (\mathbf{r},\ t)$; for a two-particle system in three dimensions, it is $\psi\ (\mathbf{r}_1,\ \mathbf{r}_2,\ t)$; and so on. In the Dirac notation an abstract state vector $|\psi(t)\rangle$ is introduced and is projected onto the appropriate space, according to the identification $\psi(x, t) = \langle x|\psi(t)\rangle$, $\psi(\mathbf{r}, t) = \langle \mathbf{r}|\psi(t)\rangle$, and so on. As will be seen shortly, $\psi(x, t)$ is a complex function (i.e., it has real and imaginary parts). The wavefunction contains all the information that may be obtained about a physical system. Unfortunately, it is now possible to write down the exact wavefunctions only for very simple systems.

According to Born's interpretation of the wavefunction, if a measurement of the position of a particle is made at time t (in the one-dimensional case), the relative probability of finding the particle between x and $x + dx$ is given by $dP = |\psi(x, t)|^2 dx$, where the square of the absolute value of ψ is taken. When possible, it is useful to normalize the probability density so that

$$\langle\psi(t)|\psi(t)\rangle \equiv \int_{-\infty}^{\infty} |\psi(x, t)|^2\, dx = 1. \tag{WC.1}$$

This states that the particle must be found somewhere, with probability 1.

The wavefunction for a particle in one dimension satisfies the Schrödinger equation

$$-\frac{\hbar^2}{2m}\frac{\partial^2\psi}{\partial x^2} + V(x)\psi = i\hbar\frac{\partial\psi}{\partial t}. \tag{WC.2}$$

Here m is the mass of the particle, $\hbar = h/2\pi = 1.0545887 \times 10^{-34}$ Js, $i = \sqrt{-1}$, and $V(x)$ is the potential energy influencing the particle's motion as it moves through space. In general, the wavefunction will be a complex function of its arguments. The Schrödinger equation is linear in ψ. Thus, if $\psi_1\ (x,\ t)$ and $\psi_2\ (x,\ t)$ are solutions, the

[†] The material on this home page is supplemental to *The Physics and Chemistry of Materials* by Joel I. Gersten and Frederick W. Smith. Cross-references to material herein are prefixed by a "W"; cross-references to material in the textbook appear without the "W."

superposition $\psi = c_1\psi_1 + c_2\psi_2$ is also a solution. This means that both constructive and destructive interference are possible for matter waves, just as for light waves.

In quantum mechanics physical quantities are represented by operators. Examples include the position, x, the momentum, $p_x = -i\hbar\partial/\partial x$, and the energy (or Hamiltonian), $H = p_x^2/2m + V(x)$, which is the sum of the kinetic energy and the potential energy operators. If a number of measurements of a physical quantity are made and the results averaged, one obtains the expectation value of the quantity. The expectation value of any physical operator, Q, is given in quantum mechanics by

$$\langle Q\rangle = \langle\psi(t)|Q|\psi(t)\rangle = \int_{-\infty}^{\infty} \psi^*(x,t)Q\psi(x,t)\,dx. \tag{WC.3}$$

To guarantee that the expectation value always be a real number, it is necessary for Q to be a Hermitian operator. A Hermitian operator is one for which the following identity holds for any two functions f and g:

$$\langle f|Qg\rangle = \langle Qf|g\rangle = \int_{-\infty}^{\infty} f^*(x)Qg(x)\,dx = \int_{-\infty}^{\infty} (Qf(x))^* g(x)\,dx. \tag{WC.4}$$

The operators x, p_x, and H are examples of Hermitian operators, as is the set of orbital angular momentum operators:

$$L_x = yp_z - zp_y, \qquad L_y = zp_x - xp_z, \qquad L_z = xp_y - yp_x. \tag{WC.5}$$

If a measurement is made of a physical variable Q, the result will be one of the eigenvalues q_i of the operator $\mathbf{Q}$, and the act of measurement will reset the wavefunction to the corresponding eigenfunction of that operator, $|q_i\rangle$. The eigenvalues and eigenfunctions are defined through the relation

$$Q|q_i\rangle = q_i|q_i\rangle. \tag{WC.6}$$

The eigenvalues of a Hermitian operator may be shown to be real numbers. Their eigenfunctions may be chosen so that they form an orthogonal set, that is,

$$\langle q_i|q_j\rangle = \int \phi^*_{q_i}(x)\phi_{q_j}(x)\,dx = \delta_{i,j}. \tag{WC.7}$$

It is customary to normalize the eigenfunctions as well, when possible. For example, the eigenfunctions of the momentum operator p_x are the plane waves $\phi_k(x) = \exp(ikx)$. They are not normalizable since it is equally probable to find the particle anywhere on the infinite domain $-\infty < x < \infty$. The corresponding momentum eigenvalue is $\hbar k$.

It is assumed that the eigenfunctions of any physical operator form a complete set (i.e., that the wavefunction may be expanded in terms of them). Thus

$$|\psi(t)\rangle = \sum_n c_n(t)|q_n\rangle. \tag{WC.8}$$

If a measurement of Q is made, the probability of finding the eigenvalue q_n is given by $|c_n|^2$. Obviously, $\sum |c_n|^2 = 1$.

A necessary and sufficient condition for a set of operators $\{Q_i\}$ to be observable simultaneously is that they commute with each other (i.e., $[Q_i, Q_j] = Q_iQ_j - Q_jQ_i = 0$). Examples of sets of commuting operators are $\{Q_1, Q_2, Q_3\} = \{x, y, z\}$, or $\{Q_1, Q_2, Q_3\} = \{p_x, p_y, p_z\}$, or $\{Q_1, Q_2\} = \{L^2, L_z\}$, where $L^2 = L_x^2 + L_y^2 + L_z^2$. Noncommuting operators may not be measured simultaneously to arbitrary accuracy. Examples include $\{Q_1, Q_2\} = \{x, p_x\}$, since $[x, p_x] = i\hbar$, or $\{Q_1, Q_2, Q_3\} = \{L_x, L_y, L_z\}$ [see Eq. (WC.22)]. When operators fail to commute, successive measurements of the respective physical variables interfere with each other. Thus measurement of x affects the outcome of a measurement of p_x. The result is summarized by the *Heisenberg uncertainty principle*, which states that the product of the uncertainties in these variables obeys the inequality $\Delta x\, \Delta p_x \geq \hbar/2$.

Stationary states of the Schrödinger equation are the analogs of standing waves in classical wave physics. They are solutions that may be expressed in factored form [i.e., $\psi(x, t) = \phi(x) \exp(-iEt/\hbar)$]. Such a state has a time-independent probability density, $|\phi(x)|^2$ and an energy E. Insertion of this expression into Eq. (WC.2) results in the time-independent Schrödinger equation,

$$H\phi(x) = E\phi(x), \tag{WC.9}$$

which shows that $\phi(x)$ is an eigenfunction of H with energy eigenvalue E.

Examples of common quantum-mechanical systems include the one-dimensional infinite square well, the simple harmonic oscillator, and the hydrogen atom. For the one-dimensional infinite square well, the potential energy operator is given by $V(x) = 0$ for $0 < x < a$ and $V(x) = \infty$ otherwise. The energy eigenfunctions are (see Table 11.5)

$$\phi_n(x) = \sqrt{\frac{2}{a}} \sin \frac{n\pi x}{a}, \tag{WC.10}$$

where $n = 1, 2, 3, \ldots$. The energy eigenvalues are

$$E_n = \frac{\hbar^2}{2m} \left(\frac{n\pi}{a}\right)^2. \tag{WC.11}$$

For the simple harmonic oscillator with frequency ω, the time-independent Schrödinger equation is given by

$$H\phi_n(x) = -\frac{\hbar^2}{2m} \frac{\partial^2 \phi_n(x)}{\partial x^2} + \frac{m\omega^2 x^2}{2} \phi_n(x) = E_n \phi_n(x). \tag{WC.12}$$

The energy eigenvalues are given by

$$E_n = \left(n + \tfrac{1}{2}\right) \hbar\omega, \tag{WC.13}$$

where $n = 0, 1, 2, \ldots$. The eigenfunctions may be expressed as products of Gaussians multiplied by Hermite polynomials:

$$\phi_n(x) = \frac{1}{2^{n/2}\sqrt{n!}} \left(\frac{m\omega}{\pi\hbar}\right)^{1/4} \exp\left(-\frac{m\omega x^2}{2\hbar}\right) H_n\left(\sqrt{\frac{m\omega}{\hbar}} x\right). \tag{WC.14}$$

The first few Hermite polynomials are $H_0(x) = 1$, $H_1(x) = 2x$, and $H_2(x) = 4x^2 - 2$.

The Schrödinger equation for the hydrogen atom is

$$-\frac{\hbar^2}{2m}\nabla^2\phi_{nlm}(\mathbf{r}) - \frac{e^2}{4\pi\epsilon_0 r}\phi_{nlm}(\mathbf{r}) = E_n\phi_{nlm}(\mathbf{r}). \tag{WC.15}$$

The energy eigenvalues for the bound states are

$$E_n = -\frac{e^2}{8\pi\epsilon_0 a_1 n^2}, \tag{WC.16}$$

where the first Bohr radius is given by $a_1 = 4\pi\epsilon_0\hbar^2/me^2$ and $n = 1, 2, 3, \ldots$. The bound-state wavefunctions are of the form

$$\phi_{nlm}(\mathbf{r}) = N_{nlm}R_{nl}(r)Y_{lm}(\theta, \phi), \tag{WC.17}$$

where $Y_{lm}(\theta, \phi)$ is a spherical harmonic (see the next paragraph). The quantum number l assume the values $0, 1, 2, \ldots, n-1$. The m quantum numbers take on the values $-l, -l+1, \ldots, l-1, l$. The ground state, with the quantum numbers $(n, l, m) = (1, 0, 0)$, is

$$\phi_{100}(\mathbf{r}) = \sqrt{\frac{1}{\pi a_1^3}}\exp\left(-\frac{r}{a_1}\right). \tag{WC.18}$$

The hydrogen atom also possesses a continuum of states for $E > 0$, which describe the Coulomb scattering of an electron from a proton.

The spherical harmonics are simultaneous eigenstates of the angular momentum operators L^2 and L_z, that is,

$$L^2Y_{lm}(\theta, \phi) = l(l+1)\hbar^2Y_{lm}(\theta, \phi), \tag{WC.19}$$

$$L_zY_{lm}(\theta, \phi) = m\hbar Y_{lm}(\theta, \phi), \tag{WC.20}$$

where θ and ϕ are spherical polar coordinates. The first few spherical harmonics are

$$\begin{aligned} Y_{00}(\theta, \phi) &= \frac{1}{\sqrt{4\pi}}, \qquad Y_{10} = \sqrt{\frac{3}{4\pi}}\cos\theta, \\ Y_{11} &= -\sqrt{\frac{3}{8\pi}}\sin\theta\, e^{i\phi}, \qquad Y_{1-1} = \sqrt{\frac{3}{8\pi}}\sin\theta\, e^{-i\phi}. \end{aligned} \tag{WC.21}$$

The angular momentum commutation relations are

$$[L_x, L_y] = i\hbar L_z, \qquad [L_y, L_z] = i\hbar L_x, \qquad [L_z, L_x] = i\hbar L_y. \tag{WC.22}$$

The spin of the electron is incorporated by writing the wavefunction as a two-component column vector. The upper and lower elements are the probability amplitudes for the electron having spin up or spin down, respectively. The operators for spin-angular momentum are written in terms of the Pauli spin matrices:

$$S_x = \frac{\hbar}{2}\sigma_x, \qquad S_y = \frac{\hbar}{2}\sigma_y, \qquad S_z = \frac{\hbar}{2}\sigma_z, \tag{WC.23}$$

where the Pauli spin matrices are given by

$$\sigma_x = \begin{pmatrix} 0 & 1 \\ 1 & 0 \end{pmatrix}, \qquad \sigma_y = \begin{pmatrix} 0 & -i \\ i & 0 \end{pmatrix}, \qquad \sigma_z = \begin{pmatrix} 1 & 0 \\ 0 & -1 \end{pmatrix}. \tag{WC.24}$$

The S_x, S_y, and S_z matrices obey the angular momentum commutation rules given in Eq. (WC.22).

Tunneling through a barrier is one of the dramatic quantum-mechanical effects. Consider a potential barrier given by $V(x) = V_0$ for $0 < x < a$ and $V(x) = 0$ otherwise. Let a particle approach it with energy $E < V_0$. The particle is able to tunnel through the barrier with some finite probability. The transmission probability is given by

$$T = \frac{1}{1 + V_0^2 \sinh^2 qa/4E(V_0 - E)}, \tag{WC.25}$$

where $q = \sqrt{2m(V_0 - E)}/\hbar$.

Time-independent perturbation theory is used to calculate the effect of a small interaction term added to the Hamiltonian. Let $H = H_0 + \lambda V$ and $H_0\phi_n = E_n^0\phi_n$ define the unperturbed eigenvalues and eigenfunctions. The quantity λ is a small parameter. Assume that the eigenvalues are nondegenerate (i.e., no two values of E_n^0 coincide). Then an approximate expression for the eigenvalues of $H\phi_n = E_n\phi_n$ is

$$E_n = E_n^0 + \lambda\langle\phi_n^0|V|\phi_n^0\rangle + \lambda^2 {\sum_j}' \frac{|\langle\phi_j^0|V|\phi_n^0\rangle|^2}{E_n^0 - E_j^0} + \cdots, \tag{WC.26}$$

where the term $j = n$ is excluded from the sum.

The case in which there is degeneracy is usually handled by matrix techniques. A finite set of eigenfunctions is chosen and the matrix elements of H are formed:

$$H_{jn} = \langle\phi_j^0|H|\phi_n^0\rangle. \tag{WC.27}$$

The eigenvalues and eigenvectors of the Hamiltonian matrix are computed. An example of this is provided by the two-level system in which the unperturbed states are labeled $|1\rangle$ and $|2\rangle$. The Hamiltonian matrix is

$$H = \begin{pmatrix} E_1 & V_{12} \\ V_{21} & E_2 \end{pmatrix}, \tag{WC.28}$$

where $V_{21} = V_{12}^*$. The eigenvalues are obtained as solutions of the secular equation

$$\begin{vmatrix} E_1 - E & V_{12} \\ V_{21} & E_2 - E \end{vmatrix} = (E_1 - E)(E_2 - E) - |V_{12}|^2 = 0 \tag{WC.29}$$

and are given by

$$E_\pm = \frac{E_1 + E_2}{2} \pm \sqrt{\left(\frac{E_1 - E_2}{2}\right)^2 + |V_{12}|^2}. \tag{WC.30}$$

The variation principle permits one to obtain an approximate solution to the Schrödinger equation and an upper bound on the energy of the ground state of a system. An arbitrary function $F(x)$ is chosen and the expectation value of the Hamiltonian is computed using this function:

$$E[F(x)] = \frac{\langle F|H|F\rangle}{\langle F|F\rangle}. \tag{WC.31}$$

Then it may be shown that the ground-state energy obeys the inequality $E_0 \leq E[F(x)]$. The function $F(x)$ depends on a set of parameters, $\{\alpha_i\}$. The parameters are varied to obtain the minimum value of $E[F(x)]$. The more parameters the function contains, the more accurately $F(x)$ will approximate the ground-state wavefunction and the closer $E[F(x)]$ will be to the ground-state energy.

In some problems there is a discrete state that is degenerate with a continuum of states. Assuming that the system starts in the discrete state, one calculates the transition rate, Γ, to the final continuum of states. Again, take the Hamiltonian to be of the form $H = H_0 + \lambda V$. The initial state satisfies $H_0|i\rangle = E_i|i\rangle$ and the final state satisfies $H_0|f\rangle = E_f|f\rangle$. The Fermi golden rule states that

$$\Gamma = \frac{2\pi}{\hbar} \sum_f |\langle f|\lambda V|i\rangle|^2 \delta(E_f - E_i). \tag{WC.32}$$

In treating systems with more than one particle, the symmetry of the wavefunction under interchange is important. For identical particles with half-integer spin, such as electrons, protons, neutrons, and ^{3}He, the wavefunction changes sign if any two particles have their positions (and spins) interchanged, that is,

$$\psi(1, \ldots, i, \ldots, j, \ldots, N) = -\psi(1, \ldots, j, \ldots, i, \ldots, N). \tag{WC.33}$$

The particles are said to obey Fermi–Dirac statistics. For identical particles with integer spin, such as photons or ^{4}He, the wavefunction is symmetric under interchange:

$$\psi(1, \ldots, i, \ldots, j, \ldots, N) = \psi(1, \ldots, j, \ldots, i, \ldots, N). \tag{WC.34}$$

Such particles obey Bose–Einstein statistics.

MATERIALS INDEX

Periodic Tables

Elements

Binary compounds and alloys

Ternary compounds and alloys

Quaternary compounds and alloys

Larger compounds, alloys, and some minerals

Polymers

Some organic molecules

INDEX